Energy Technology Division
Energy Technology Division
Energy Technology Division
Energy Technology Division
Energy Technology Division
Energy Technology Division
Energy Technology Division
Energy Technology Division
Energy Technology Division
Energy Technology Division
Energy Technology Division
Energy Technology Division
Energy Technology Division
Energy Technology Division
Energy Technology Division
Energy Technology Division
Energy Technology Division
Energy Technology Division
Energy Technology Division
Energy Technology Division
Energy Technology Division
Energy Technology Division
Energy Technology Division
Energy Technology Division
Energy Technology Division
Energy Technology Division
Energy Technology Division
Energy Technology Division
Energy Technology Division
Energy Technology Division
Energy Technology Division
Energy Technology Division
Energy Technology Division

ANL-95/9

Boiling Heat Transfer with Three Fluids in Small Circular and Rectangular Channels

by T. N. Tran, M. W. Wambsganss, and D. M. France

Argonne National Laboratory, Argonne, Illinois 60439
operated by The University of Chicago
for the United States Department of Energy under Contract W-31-109-Eng-38

Energy Technology Division
Energy Technology Division
Energy Technology Division
Energy Technology Division
Energy Technology Division
Energy Technology Division
Energy Technology Division
Energy Technology Division

Reproduced from the best available copy.

Available to DOE and DOE contractors from the
Office of Scientific and Technical Information
P.O. Box 62
Oak Ridge, TN 37831
Prices available from (615) 576-8401

Available to the public from the
National Technical Information Service
U.S. Department of Commerce
5285 Port Royal Road
Springfield, VA 22161

DISCLAIMER

ARGONNE NATIONAL LABORATORY
9700 South Cass Avenue, Argonne, Illinois 60439

ANL–95/9

Distribution Category:
Thermal Science
(UC–1423)

Boiling Heat Transfer with Three Fluids in Small Circular and Rectangular Channels

by

T. N. Tran, M. W. Wambsganss, and D. M. France[1]

Energy Technology Division

[1]Department of Mechanical Engineering (m/c 251), University of Illinois at Chicago, 842 W. Taylor St., Rm. 2039, Chicago, IL 60607-7022.

January 1995

Work supported by

U. S. DEPARTMENT OF ENERGY
Office of Energy Efficiency and Renewable Energy

Contents

Nomenclature vi

Abstract 1

1 Introduction 2

2 Test Apparatus and Instrumentation 4

3 Test Procedure and Data Reduction 6

4 Experimental Results 7

4.1 Rectangular Channel, R-12 Boiling Fluid 8
4.2 Circular Tube, R-12 Boiling Fluid 10
4.3 Circular Tube, R-134a Boiling Fluid 12

5 Discussion 15

5.1 Heat Transfer Mechanisms 15
5.2 Effect of Flow Channel Geometry 17
5.3 Comparison with Large Tubes 18
5.4 Correlation of Data 22
5.5 Comparison of R-12 and R-134a 24

6 Summary and Conclusions 25

Acknowledgments 27

References 27

Appendix: Small Channel Flow Boiling Data 31

Figures

1 Schematic diagram of test apparatus 4

2 Circular tube test section showing locations of instrumentation 5

3 Rectangular channel (R-12) local heat transfer for various combinations of mass flux at approximately constant values of heat flux and $\Delta T_{sat} > 2.75°C$ 8

4 Rectangular channel (R-12) average heat transfer coefficient as a function of mass flux for select values of approximately constant heat flux and $\Delta T_{sat} > 2.75°C$ 9

5 Rectangular channel (R-12) heat flux dependence on wall superheat... 9

6 Rectangular channel (R-12) heat transfer 10

7 Circular tube (R-12) local heat transfer results for various combinations of mass flux at approximately constant values of heat flux and $\Delta T_{sat} > 2.75°C$ 11

8 Circular tube (R-12) average heat transfer coefficient as a function of mass flux for select values of approximately constant heat flux and $\Delta T_{sat} > 2.75°C$ 11

9 Circular tube (R-12) heat flux dependence on wall superheat 12

10 Circular tube (R-12) effect of saturation pressure in nucleation-dominant boiling region 13

11 Circular tube (R-12) convection-dominant heat transfer at low wall superheat 13

12 Circular tube (R-134a) average heat transfer coefficient as a function of mass flux for select values of approximately constant heat flux and $\Delta T_{sat} > 2.75°C$ 14

13 Circular tube (R-134a) heat flux dependence on wall superheat 14

14 Circular tube (R-134a) convection-dominant boiling 15

15 Heat transfer behavior of small rectangular and circular channels with pool boiling prediction of Stephan and Abdelsalam.................... 18

16 Large tube comparison with circular channel data for R-12 using Kandlikar correlation.. 19

17 Quality effect on large tube comparison with rectangular channel data.. 20

18 Large tube comparison with circular channel data for R-12 using Jung and Radermacher correlation... 21

19 Large tube comparison with circular channel data for R-12 using Liu and Winterton correlation.. 22

20 Transition temperatures.. 22

21 Heat transfer predictions of Eq. 4 for rectangular channel (R-12)......... 23

22 Heat transfer predictions of Eq. 4 for circular tube (R-12)................... 23

23 Correlation of round tube data for three fluids at $\Delta T_{sat} > 2.75°C$........... 25

24 Heat transfer behavior of R-134a and R-12 in nucleation-dominant region in 2.46-mm-diameter round tube... 26

Tables

1 Parameter ranges for all tests... 7

2 Parameter ranges for tests with $\Delta T_{sat} > 2.75°C$ 7

3 Correlation coefficients for R-12 17

A.1 Circular Tube (d = 2.92 mm); R-113.. 33

A.2 Circular Tube (d = 2.46 mm); R-12 34

A.3 Circular Tube (d = 2.46 mm); R-134a 38

A.4 Rectangular Tube (d_h = 2.40 mm); R-12 40

Nomenclature

A	Channel cross-sectional flow area (m^2)
Bo	Boiling number ($= q''/i_{fg}G$)
C_1	Coefficient in Eq. 3
C_2	Coefficient in Eq. 3
C_3	Coefficient in Eq. 4
C_4	Coefficient in Eq. 4
d	Diameter of circular tube (m)
G	Mass flux (kg/m^2s)
h	Heat transfer coefficient ($W/m^2{}^\circ C$)
i_{fg}	Latent heat of evaporation (J/kg)
L_H	Heated length (m)
L_{SB}	Subcooled length (m)
P	Pressure (kPa)
P_R	Reduced pressure
q''	Surface heat flux (W/m^2)
Q_E	Heat transfer rate based on electric power input (W)
S	Channel circumference (m)
T_{sat}	Saturation temperature (°C)
T_w	Wall temperature (°C)
x	Equilibrium mass quality; Eq. (2)
We_ℓ	Weber number based on liquid ($= G^2 d/\rho_\ell \sigma$)
z	Distance along channel from start of boiling
η	Heat loss factor
ρ_ℓ	Liquid density (kg/m^3)
ρ_v	Vapor density (kg/m^3)
σ	Surface tension (N/m)
ΔT_{sat}	Wall superheat, $T_w - T_{sat}$ (°C)

Boiling Heat Transfer with Three Fluids in Small Circular and Rectangular Channels

by

T. N. Tran, M. W. Wambsganss, and D. M. France[1]

Abstract

Small circular and noncircular channels are representative of flow passages in compact evaporators and condensers. This report describes results of an experimental study on heat transfer to the flow boiling of refrigerant-12 (R-12) and refrigerant-134a (R-134a) in a small horizontal circular-cross-section tube. The tube diameter of 2.46 mm was chosen to approximate the hydraulic diameter of a 4.06 x 1.70 mm rectangular channel previously studied with R-12, and a 2.92-mm-diameter circular tube previously studied with R-113. The objective of this study was to assess the effects of channel geometry and fluid properties on the heat transfer coefficient and to obtain additional insights relative to the heat transfer mechanism(s). The current circular flow channel for the R-12 and R-134a tests was made of brass and had an overall length of 0.9 m. The channel wall was electrically heated, and thermocouples were installed on the channel wall and in the bulk fluid stream. Voltage taps were located at the same axial locations as the stream thermocouples to allow testing over an exit quality range to 0.94 and a large range of mass flux (58 to 832 kg/m^2s) and heat flux (3.6 to 59 kW/m^2). Saturation pressure was nearly constant, averaging 0.82 MPa for most of the testing, with some tests performed at a lower pressure of 0.4-0.5 MPa. Local heat transfer coefficients were determined experimentally as a function of quality along the length of the test section. Analysis of all data for three tubes and three fluids supported the conclusion that a nucleation mechanism dominates for flow boiling in small channels. Nevertheless, a convection-dominant region was obtained experimentally in this study at very low values of wall superheat ($<\approx 2.75°C$). The circular and rectangular tube data for three fluids were successfully correlated in the nucleation-dominant region. After comparison of the measured heat transfer coefficients for the circular and rectangular channels, we concluded that for channels with the same hydraulic diameter, in the range tested, geometry did not have an appreciable influence on heat transfer coefficient, but heat transfer rates were higher in both cases than would be predicted for larger-diameter channels.

---

[1]Department of Mechanical Engineering (m/c 251), University of Illinois at Chicago, 842 W. Taylor St., Rm. 2039, Chicago, IL 60607-7022.

1 Introduction

Compact heat exchangers have been defined as having a surface-area density ratio greater than 700 m^2/m^3 (Shah 1986); for a circular tube, this translates to a diameter of <6 mm. The higher heat transfer surface-area density inherent in compact heat exchangers allows significantly higher heat flux levels to be attained relative to two-phase flows in conventional circular tube exchangers. An additional consideration with compact evaporators is the effect of flow passage geometry and size on the two-phase flow and heat transfer phenomena. For example, in the noncircular passages of compact evaporators, geometry may influence the liquid inventory (flow pattern) at a given cross section via surface tension and capillary force action.

Studies reporting in the open literature on vaporization in compact heat exchangers are relatively few. They can conveniently be grouped as exchangers with offset strip fin passages (Panitsidis et al. 1975; Galezha et al. 1976; Yung et al. 1980; Chen and Westwater 1984), exchangers with perforated fin passages (Panchal 1984, 1989), multichannel arrangements with offset strip fins (Robertson, 1979, 1983; Carey and Mandrusiak 1986; Mandrusiak et al. 1988; Mandrusiak and Carey 1989), and multichannel arrangements with perforated fins (Robertson and Wadekar 1988; Wadekar 1992). Single-channel studies of flow boiling of refrigerant-113 (R-113) in a small-diameter circular tube (approximately 3 mm) have been reported by Lazarek and Black (1982) and Wambsganss et al. (1993). Boiling in single, small rectangular passages has been reported by Tran et al. (1993) and Peng and Wang (1993). In particular, Tran et al. (1993) studied flow boiling of refrigerant-12 (R-12) in a 4.06 x 1.70 mm rectangular channel, while Peng and Wang (1993) reported on flow boiling of water in an 0.6 x 0.7 mm rectangular passage.

Relative to the dominant heat transfer mechanism, results from tests on actual heat exchangers (Galezha et al. 1976; Chen and Westwater 1984; Panchal 1984) suggested a nucleation-dominant mechanism. Galezha et al. (1976) showed heat transfer coefficients to vary with heat flux, and Panchal (1984) showed heat transfer coefficients to be insensitive to flow rate. On the other hand, investigations with multipassage arrangements (Robertson, 1979, 1983; Carey and Mandrusiak 1986; Mandrusiak et al. 1988; Mandrusiak and Carey 1989; Robertson and Wadekar 1988; Wadekar 1992) all showed nucleation not to be an important mechanism. The heat transfer coefficients were independent of heat flux, dependent on mass flux, and increased with quality (all of which are features of forced convective boiling). This apparent contradiction will be reconciled, in part, by the results of this study.

Investigators of boiling in small smooth channels (circular and rectangular) (Wambsganss et al. 1993, Tran et al. 1993, Peng and Wang 1993) all concluded that a nucleation mechanism dominates. For the range of parameters tested, the measured heat transfer coefficients were effectively independent of mass flux and quality and were dependent on heat flux.

It is recognized that the dominant heat transfer mechanism is determined, in part, by the range of test conditions employed and that this can be expected to contribute to the explanation of the differences in conclusions reached by different researchers. However, it is also clear that to generate the technology base required for the development of design methods and standards for boiling in the flow passages of compact evaporators, there is a need to better understand these mechanisms and their transitions.

In addition to improving the understanding of fundamental heat transfer mechanisms, the potential for enhancing heat transfer by optimizing passage cross-sectional geometries is of significant interest to designers. In this regard, Tran et al. (1993) suggested that heat transfer may be more efficient in a small rectangular channel than in a circular channel of approximately the same hydraulic diameter. This was based on the fact that state-of-the-art correlations for in-tube evaporation that did well in correlating the small-circular-tube data of Wambsganss et al. (1993) were shown to significantly underpredict the small-rectangular-channel data (Tran et al. 1993).

Additional flow boiling data were obtained with R-12 in a 4.06 x 1.70 mm (hydraulic diameter d_h = 2.44 mm) rectangular brass channel and are presented here. These data supplement the data presented in Wambsganss et al. (1993). In the present study, flow boiling heat transfer with R-12 and R-134a in a circular 2.46 mm i.d. brass tube was investigated. The circular tube diameter of 2.46 mm was selected to closely match the rectangular channel hydraulic diameter of 2.40 mm, thus allowing a more direct evaluation of the effect of channel geometry on heat transfer. R-12 tests in the circular tube were performed over a range of test conditions that facilitates direct comparison with the rectangular channel and direct evaluation of the effect of passage geometry. The lower end of the range of heat flux (and wall superheat) was also extended in order to identify a convective boiling region and provide information on the associated convective/nucleate boiling transition. Heat transfer results from the two different tube passage geometries are compared, and the R-12 results from the 2.46 mm circular tube are compared with state-of-the-art in-tube evaporation correlations developed for large tubes.

Experiments with R-134a were performed in the same circular brass channel used for the R-12 tests. The results, along with R-113 data obtained previously, were used to assess the effects of different refrigerant properties on the boiling heat transfer rates. The R-134a data are presented in this report and compared to results from the other two fluids. A single correlation equation was developed to predict the heat transfer well in the nucleation-dominant region for all of the data, including two tube cross sections (circular and rectangular) and three fluids, for the circular-tube data for all three fluids. The results presented in the Appendix include the nucleation-dominant data, upon which the correlation was based, and the convection-dominant data.

2 Test Apparatus and Instrumentation

The test apparatus and test procedure have already been described in some detail by Wambsganss et al. (1993) and Tran et al. (1993). Consequently, they are only summarized here for completeness.

The test apparatus shown in Fig. 1 is a closed-loop system with system pressure controlled by high-pressure nitrogen via a pressure regulator and a bladder-type accumulator. The fluid enters the test section in a subcooled state and is evaporated in the test section to a quality of ≈80% or lower in most tests, depending on mass flux and heat flux. The two-phase mixture leaving the test section is condensed and subcooled before entering the pump. Flow rate is measured with a constant-displacement flowmeter with an accuracy of better than 2% of the reading.

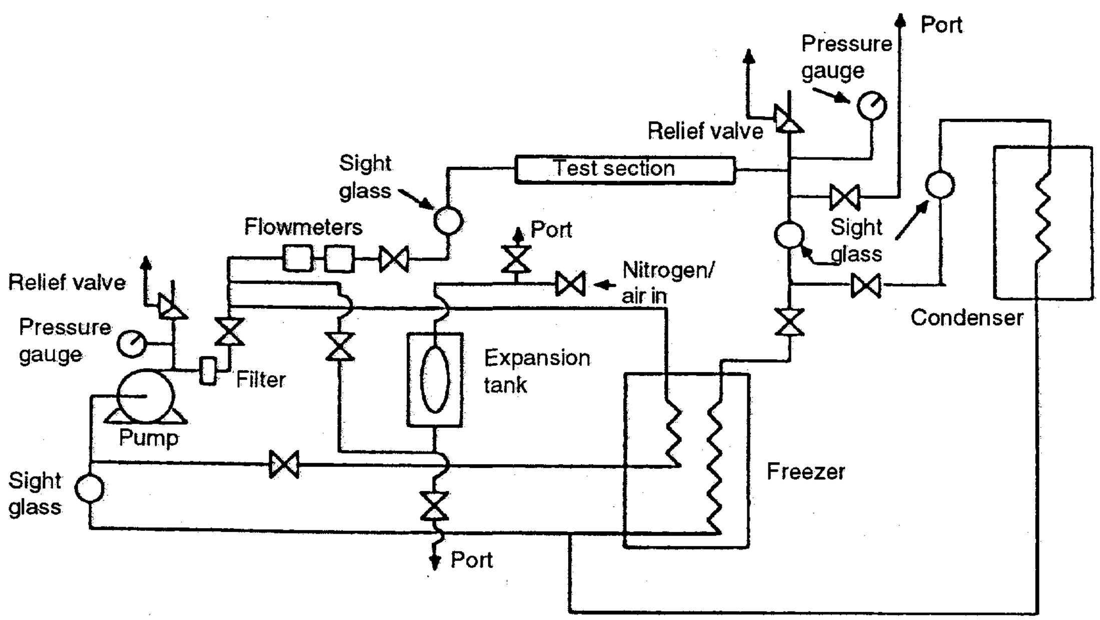

Fig. 1. Schematic diagram of test apparatus

Based on results of previous investigations (Wambsganss et al. 1993; Tran et al. 1993; Peng and Wang 1993), nucleation (which in pool boiling is a function of channel material and surface finish, as well as heat flux) is expected to be the dominant heat transfer mechanism. To eliminate possible effects of tube material on heat transfer, both the 4.06 x 1.70 mm rectangular channel and the 2.46 mm circular tube were fabricated from brass, and to minimize effects of surface conditions, both were obtained from the same tubing supplier. The two flow channels each have an overall length of 0.9 m. The channels were resistance-heated by passing a DC current through the channel wall. Heat input to the fluid was determined from the electric power input to the channel, accounting for heat losses to the environment. Figure 2 is a schematic diagram of the circular tube flow channel used in this investigation for boiling refrigerants R-12 and R-134a.

In-flow temperatures of the bulk fluid were measured at four axial locations: the inlet and outlet, and near two intermediate current clamps. Pressure ports and voltage taps were also provided at each of these four locations. Both inlet pressure and a two-phase pressure drop were measured. Wall temperatures were measured at various axial locations along the length of the channels by surface-mounted thermocouples for the rectangular tube and by surface-mounted resistance temperature devices (RTDs) for the circular tube. Liquid tests (isothermal and heat balance) were used to establish uncertainty in temperature measurements of ±0.25°C.

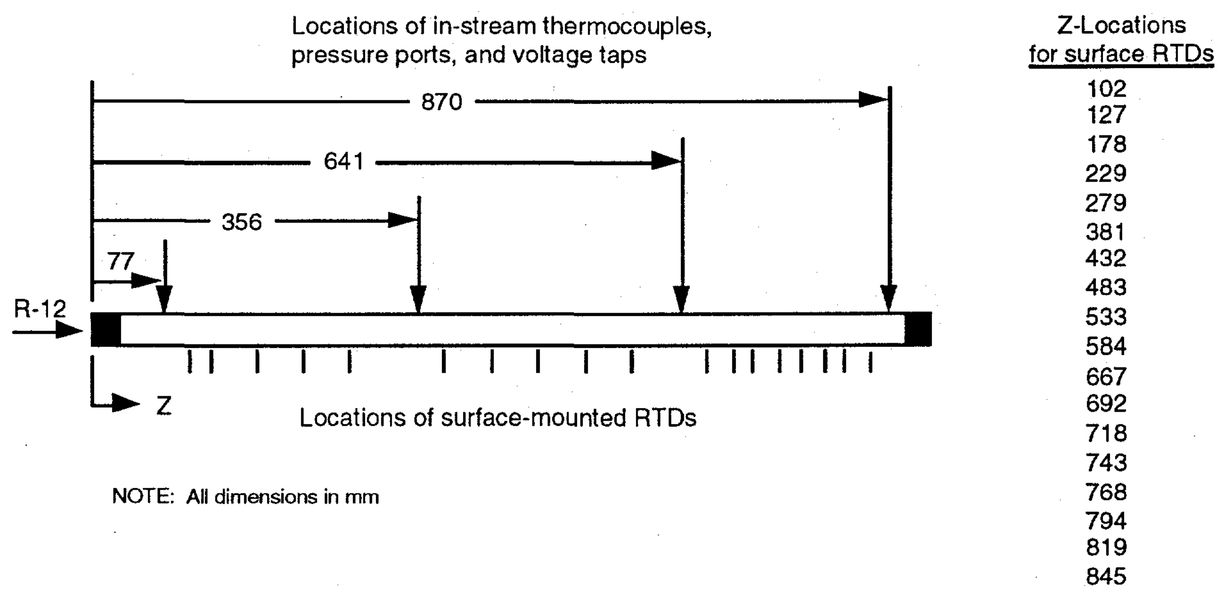

Fig. 2. Circular tube test section showing locations of instrumentation (RTD = resistance temperature device)

3 Test Procedure and Data Reduction

As with the test apparatus and instrumentation discussed in the preceding section, the test procedure and data reduction methodology have already been described in detail by Wambsganss et al. (1993) and Tran et al. (1993) and are only summarized here for completeness.

Single-phase tests were first performed to provide (1) an overall system check of instrumentation, calibration, and data acquisition equipment and techniques, and (2) a determination of heat loss to the environment. Subsequently, a series of flow boiling tests was conducted at constant values of mass flux and selected values of heat flux.

The local evaporative heat transfer coefficient was calculated as

$$h(z) = \frac{q''}{T_w(z) - T_{sat}(z)}, \quad (1)$$

where $q'' = \eta Q_E / S(L_H - L_{SB})$. The quality at the measurement location z was calculated as

$$x(z) = \frac{S(z - L_{SB})q''}{AGi_{fg}}. \quad (2)$$

In Eq. 1, the wall temperatures were measured directly while the saturation temperatures were obtained indirectly—from a two-phase pressure drop and exit saturation temperature measurement—following a procedure outlined in Tran et al. (1993). In some cases, a temperature measurement centered in the two-phase region served to verify the accuracy of this procedure.

For each of the steady-state tests corresponding to a specific mass flux and heat flux, local heat transfer coefficients were determined for a range of qualities along the length of the test section. In virtually all cases, the heat transfer coefficients were effectively independent of quality for qualities greater than 20%. Results showing this effect will be presented for the rectangular channel with R-12 and for the circular tube with both R-12 and R-134a. In the test results presented subsequently, average heat transfer coefficients—obtained as the average of the measured local heat transfer coefficients for qualities greater than 20%—are given. Average wall superheats for given test runs are also calculated and used in the presentation of results. The product of the averaged heat transfer coefficient h and averaged wall superheat ΔT_{sat} is equal to the heat flux q".

4 Experimental Results

Including data reported by Tran et al. (1993), 132 tests for the rectangular channel are reported here; 204 new tests for the circular tube are reported, of which 137 were performed with R-12 and 67 with R-134a. Test data are given in the Appendix. Table 1 gives the test parameter ranges for all tests. As discussed later, a wall superheat of approximately 2.75°C was determined to approximate the threshold between the convective and nucleate boiling regions; the test parameter ranges given in Table 2 are for the nucleate boiling region.

Table 1. Parameter ranges for all tests

Fluid	No. of Tests	Channel Geometry/Size (mm)	P_R	G (kg/m^{2}s)	q" (kW/m^2)	Bo	ΔT_{sat} (°C)
R-12	137	Circular d = 2.46	0.12 & 0.20	63-832	3.6-59.5	0.00020-0.0017	1.2-6.6
R-113	27	Circular d = 2.92	≈0.045	50-400	8.8-90.8	0.00075-0.0023	7.2-18.2
R-134a	67	Circular d = 2.46	0.10 & 0.20	58-476	4.4-47.5	0.00026-0.00081	1.5-6.0
R-12	132	Rectangular 1.70 x 4.06 d_h = 2.40	≈0.20	44-505	5.6-129	0.00028-0.0016	1.8-8.2

Table 2. Parameter ranges for tests with ΔT_{sat} > 2.75°C

Fluid	No. of Tests	Channel Geometry/Size (mm)	P_R	G (kg/m^{2}s)	q" (kW/m^2)	Bo	ΔT_{sat} (°C)
R-12	104	Circular 2.46	0.12 & 0.20	63-832	7.5-59.5	0.00020-0.0017	2.8-6.6
R-113	27	Circular 2.92	≈0.045	50-400	8.8-90.8	0.00075-0.0023	7.2-18.2
R-134a	41	Circular 2.46	0.10 & 0.20	112-476	10.3-47.5	0.00039-0.00081	2.8-6.0
R-12	118	Rectangular 1.70 x 4.06 d_h = 2.40	≈0.20	44-505	7.7-129	0.00028-0.0016	2.8-8.2

An important feature of the test program is that the heat transfer tests were performed so as to isolate the effects of heat flux, mass flux, and quality; typically, data reported in the open literature do not readily allow one to isolate these effects. In particular, tests were performed for selected values of mass flux with various heat flux levels, as well as for selected values of heat flux with various mass flux levels.

4.1 Rectangular Channel, R-12 Boiling Fluid

Results from tests with the 4.06 x 1.70 mm rectangular channel are given in Figs. 3-5 for wall superheats above 2.75°C. In Fig. 3, measured local heat transfer coefficients are plotted as a function of quality for two values of constant heat flux (15.8 and 30.0 kW/m^2), and six different values of mass flux, covering a threefold range of 85 to 354 kg/m^{2}s. It can be observed from the figure that the local heat transfer coefficient is effectively independent of quality for qualities in the range of 20 to 80%; this observation supports the use of an average heat transfer coefficient over that quality range. Mass flux independence is also indicated by the data in Fig. 3.

Average heat transfer coefficients are plotted in Fig. 4 as a function of mass flux for five different constant values of heat flux. The results indicate a strong heat flux dependence and, again, essentially no mass flux dependence.

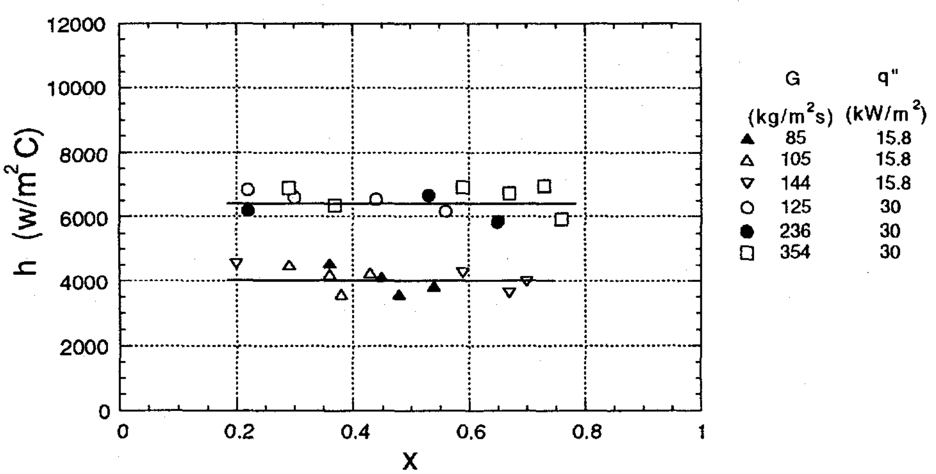

Fig. 3. Rectangular channel (R-12) local heat transfer for various combinations of mass flux at approximately constant values of heat flux and $\Delta T_{sat} > 2.75°C$

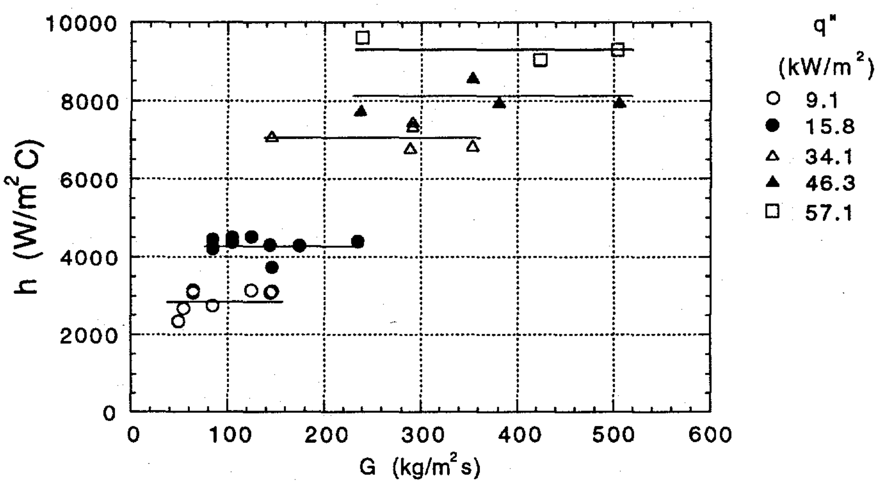

Fig. 4. Rectangular channel (R-12) average heat transfer coefficient as a function of mass flux for select values of approximately constant heat flux and $\Delta T_{sat} > 2.75$ °C

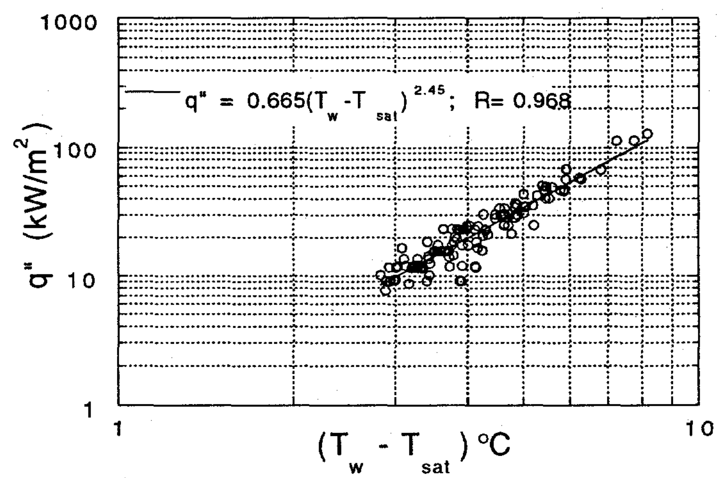

Fig. 5. Rectangular channel (R-12) heat flux dependence on wall superheat ($\Delta T_{sat} > 2.75$ °C)

In Fig. 5, heat flux is plotted as a function of average wall superheat for all tests having wall superheat >2.75°C. The data can be correlated approximately with a straight line when plotted on log-log coordinates, thus indicating a power function relationship between heat flux and wall superheat. Such a functional fit to the data is shown in Fig. 5, where the correlation coefficient R = 0.968. Heat flux is determined to vary with wall superheat raised to the 2.45 power.

Although the data of Fig. 5 show only a heat flux contribution to the heat transfer and no mass flux effect, it is expected that there is a parameter regime where the two phenomena contribute to heat transfer in small channels as they do in larger channels. To confirm this, several tests were performed in the rectangular channel at wall superheats below 2.75°C. The results, shown in Fig. 6, indicate that the lower wall superheats moved the system into a regime where mass flux effects became important. The slope of the data changes in the lower wall superheat range and there is a distinct influence of mass flux. The major difference between these data and those from large tubes is the wall superheat at which the transition occurs to heat-flux-dominant. This point will be discussed further with respect to the circular-tube data.

4.2 Circular Tube, R-12 Boiling Fluid

Results from tests with the 2.46 mm circular tube using R-12 as the boiling fluid are presented in Figs. 7-9 for wall superheats above 2.75°C. These three figures correspond to Figs. 3-5, respectively, for the rectangular channel with the same fluid. Again, the local heat transfer coefficient was only weakly dependent on quality (see Fig. 7), allowing for computation of an average heat transfer coefficient. The data in Fig. 8, showing average heat transfer coefficient as a function of mass flux for various values of heat flux, clearly indicate that for the range of heat fluxes tested, the heat transfer coefficient is effectively independent of mass flux.

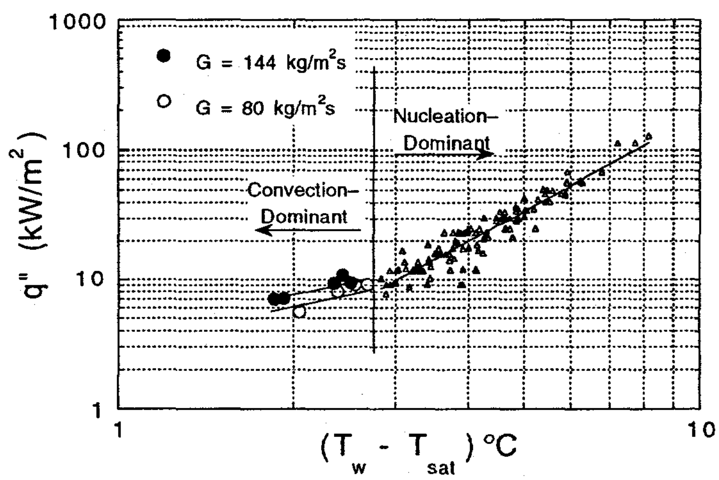

Fig. 6. Rectangular channel (R-12) heat transfer: convection region ○ - G = 80 kg/m²s; ● - G=144 kg/m²s; nucleation region ▲ - all values of mass flux tested

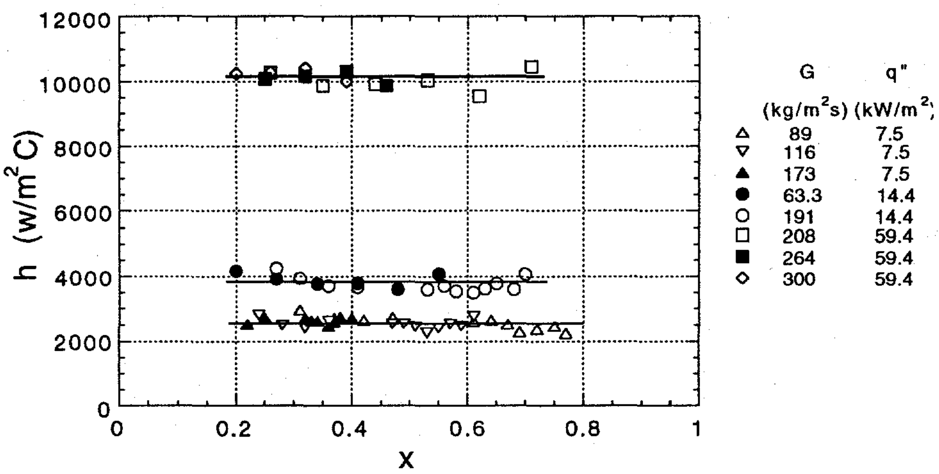

Fig. 7. Circular tube (R-12) local heat transfer results for various combinations of mass flux at approximately constant values of heat flux and $\Delta T_{sat} > 2.75°C$

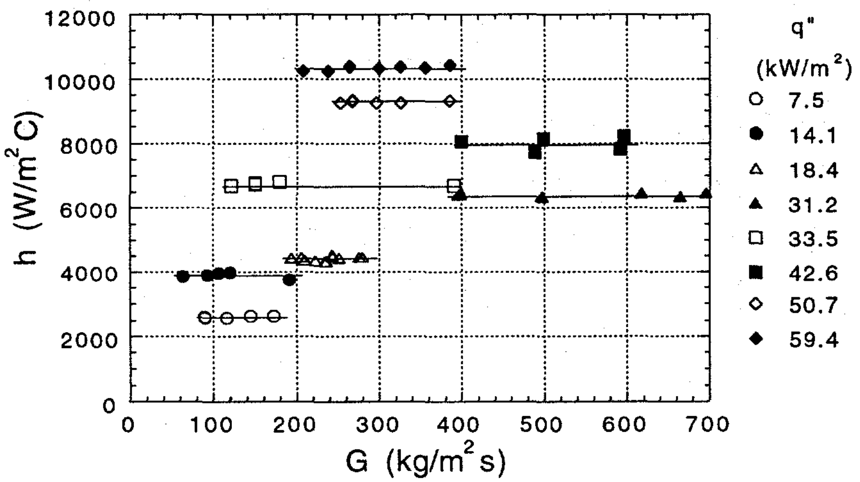

Fig. 8. Circular tube (R-12) average heat transfer coefficient as a function of mass flux for select values of approximately constant heat flux and $\Delta T_{sat} > 2.75°C$

In Fig. 9, data from the circular-tube tests are plotted in terms of heat flux and average wall superheat. As for the rectangular channel, the data can be correlated approximately with a straight line on log-log coordinates, indicating a power function relationship between heat flux and wall superheat for $\Delta T_{sat} >$ 2.75°C (as shown in the figure). In this case, the correlation coefficient R = 0.962, and the heat flux is shown to vary with wall superheat raised to the 2.71 power.

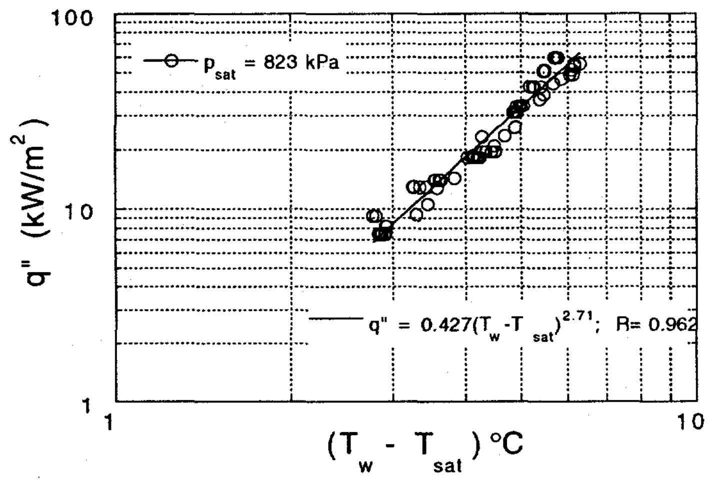

Fig. 9. Circular tube (R-12) heat flux dependence on wall superheat ($\Delta T_{sat} > 2.75$°C)

Two additional test series were performed with the circular tube: the first at a different (lower) value of saturation pressure, and the second at very low values of heat flux for two different values of mass flux. Figure 10 shows the effect of saturation pressure; heat transfer rate is proportional to saturation pressure. Figure 11 shows the results of tests performed at two different values of mass flux (72 and 150 kg/m^{2}s) to extend the data base to lower values of heat flux. At the lower values of heat flux, two distinct curves (each having a slope of approximately 1 on log-log coordinates) corresponding to each of the two values of mass flux tested can be identified. These mass-flux-dependent results are similar to those shown in Fig. 6 for the rectangular channel at low wall superheat below 2.75°C.

4.3 Circular Tube, R-134a Boiling Fluid

Tests were repeated in the 2.46 mm circular tube using R-134a as the boiling fluid. Results are shown in Figs. 12-14 for wall superheats above 2.75°C. The results shown in Fig. 12 are comparable to those of Figs. 4 and 8, where for wall superheat greater than 2.75°C it is clear that heat transfer is independent of mass flux.

The results presented in Fig. 13 for R-134a are similar to those shown in Figs. 9-11 for R-12 in the same circular tube. All of the R-134a data are plotted in Fig. 13, and the dependence of heat flux but not mass flux is evident at wall superheat above 2.75°C. At lower wall superheats, a mass flux dependence appears, as seen for R-12 in Figs. 6 and 11 for the rectangular and circular

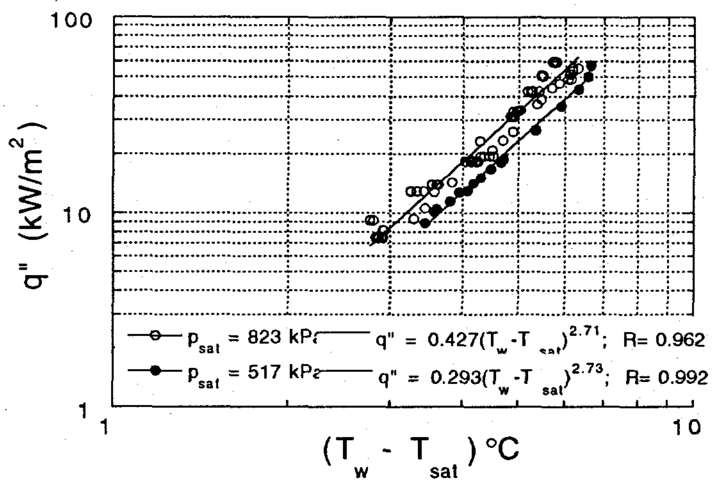

Fig. 10. Circular tube (R-12) effect of saturation pressure in nucleation-dominant boiling region; ○ *-* p_{sat} *= 0.82 MPa;* ● *-* p_{sat} *= 0.52 MPa*

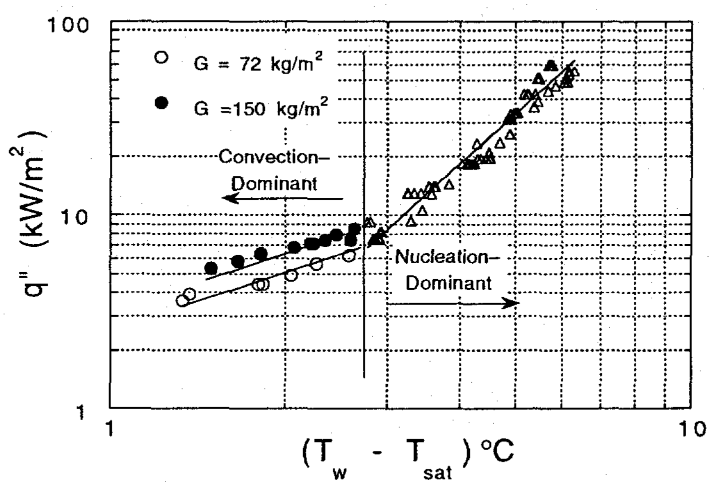

Fig. 11. Circular tube (R-12) convection-dominant heat transfer at low wall superheat: convection region ○ *-* $G = 72\ kg/m^2s$*;* ● *-* $G = 150\ kg/m^2s$*; nucleation region* ▲ *- all values of mass flux tested*

channels, respectively. The low-wall-superheat results of Fig. 13 are shown in Fig. 14 on an expanded scale and the mass flux dependence is clear. The curves converge to the nucleation-dominant condition as in larger tubes, but as with the other fluids and geometries tested, the wall superheat at transition is quite low in the case of the small channels.

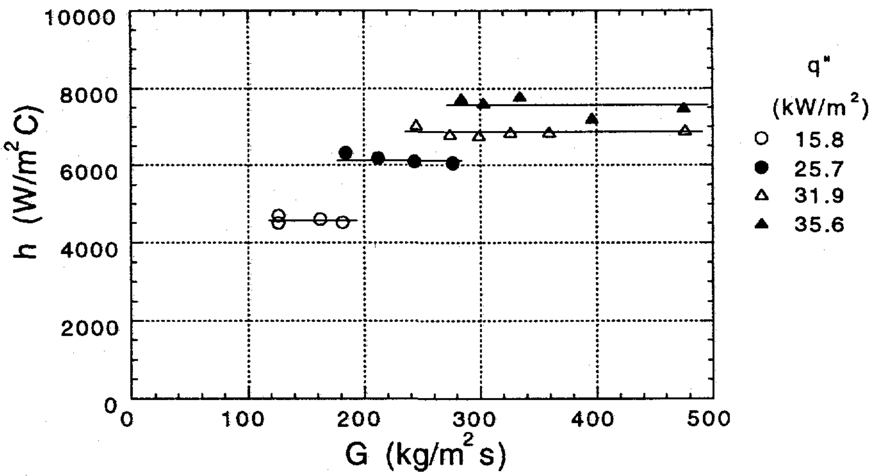

Fig. 12. Circular tube (R-134a) average heat transfer coefficient as a function of mass flux for select values of approximately constant heat flux and $\Delta T_{sat} > 2.75\,°C$

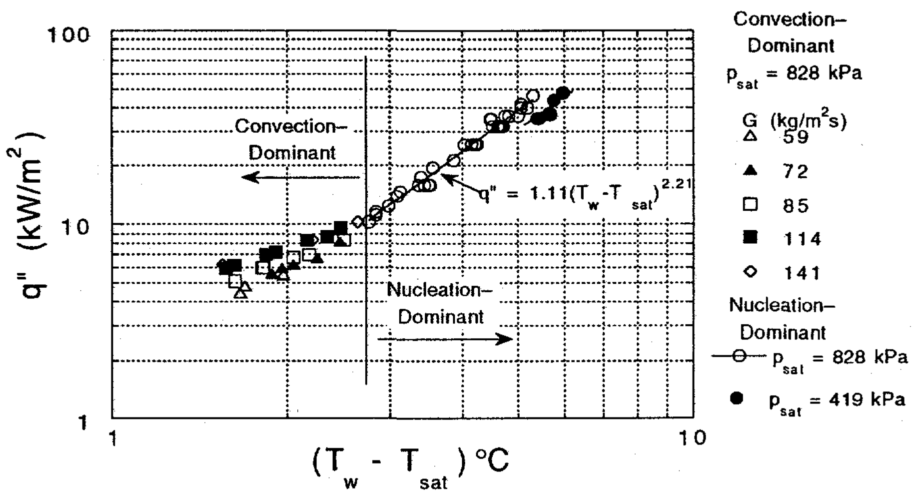

Fig. 13. Circular tube (R-134a) heat flux dependence on wall superheat

Limited data were obtained with R-134a at a lower pressure than that in the majority of the tests. These results are also shown in Fig. 13, where the trend is comparable to the R-12 results of Fig. 10; lower pressure reduces heat transfer at fixed wall superheat.

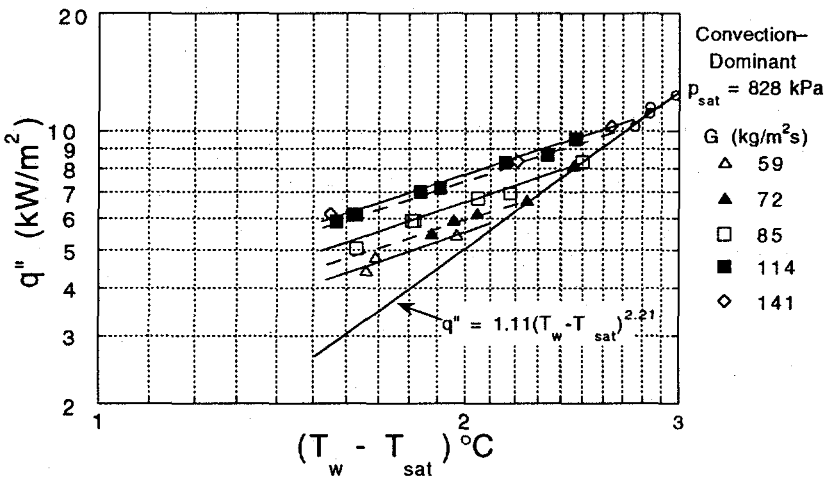

Fig. 14. Circular tube (R-134a) convection-dominant boiling

5 Discussion

The primary objectives of this investigation were to (1) further improve our understanding of the boiling heat transfer mechanisms in small channels typical of compact heat exchangers, (2) evaluate the effect of flow channel geometry on heat transfer enhancement, (3) compare small channel heat transfer behavior with that of large tubes, and (4) develop correlations for heat transfer rates in small channels for a variety of boiling fluids. A secondary objective is to compare the test results for R-12 with its replacement, R-134a. Each of these subjects is discussed below.

5.1 Heat Transfer Mechanisms

The two fundamental boiling heat transfer mechanisms are forced convection and nucleation. In forced convective boiling, the heat transfer coefficient is independent of heat flux and dependent on mass flux and quality; heat transfer increases with increasing mass flux and quality. On the other hand, when nucleation dominates, heat transfer is independent of mass flux and quality, dependent on heat flux and sensitive to saturation pressure level.

With these definitions, the results shown in Figs. 3, 4, 7, 8, and 12 lead one to conclude that over a broad range of heat flux, and in channels of two different geometries with three different fluids, nucleation is the dominant heat transfer mechanism for flow boiling in the small passages considered in this study. This agrees with previous investigations of flow boiling in small channels (Lazarek and Black 1982; Wambsganss et al. 1993; Tran et al. 1993; Peng and Wang 1993). The results shown in Figs. 10 and 13 show that saturation pressure has a measurable effect on heat transfer, decreasing the heat transfer coefficient with decreasing pressure. Because this sensitivity and trend is expected of nucleation-dominant heat transfer, it also serves to support the conclusion that a nucleation mechanism dominates.

It has been shown that a nucleation mechanism dominates over a broad range of heat flux values. Nevertheless, it was expected that at sufficiently low values of heat flux (very low wall superheat), forced convection will dominate. This was indeed shown to be the case, as illustrated in Figs. 6, 11, and 14. At wall superheats of less than 2.75°C, the boiling curve is a function of mass flux and the slope of the curve is approximately unity, implying that the heat transfer coefficient is independent of heat flux. This result is clear in the tests with R-12 and R-134a and for circular and rectangular channels where these low wall-superheat tests were performed.

The transition from convection- to nucleation-dominant boiling is well-defined and relatively abrupt for the small channel data of Figs. 6, 11, and 14. This abrupt behavior was clearly evident in the data obtained as the system became quasistable at transition, abruptly changing from convection- to nucleation-dominant. This behavior differs from that found with larger-diameter channels in which relatively broad transition regions occur, typically with contributions from both convective and nucleate boiling being important.

Identification of a convection-dominant region in small channel boiling heat transfer allows one to reconcile an apparent disagreement between the results of this investigation and the results of others who found a nucleation-dominant mechanism (Lazarek and Black 1982; Wambsganss et al. 1993; Tran et al. 1993; Peng and Wang 1993), and the results of Robertson and coworkers (Robertson 1979, 1983; Robertson and Wadekar 1988; Wadekar 1992) who concluded from their tests with multichannel arrangements that nucleation is not an important mechanism. The finding of Robertson and coworkers that convection dominates was based on data obtained for very low values of wall superheat (<2.5°C), and indeed the results presented in this paper for very low wall superheats, also lead to this conclusion. It remains to reconcile differences in conclusions by Carey and coworkers (Carey and Mandrusiak 1986; Mandrusiak et al. 1988; Mandrusiak and Carey 1989) relative to the dominant mechanism.

5.2 Effect of Flow Channel Geometry

Nucleation-dominant heat transfer data from the rectangular channel and circular tube, both with R-12, were plotted on log-log coordinates as heat flux versus wall superheat in Figs. 5 and 9, respectively. As shown in those figures, the reasonable correlation of the data with a straight line suggests a power function relationship between heat flux and wall superheat. Therefore, a dimensional prediction equation was written of the form

$$q'' = C_1(T_w - T_{sat})^{C_2}, \tag{3}$$

where q" is heat flux in kW/m^2, and T_w and T_{sat} are tube-wall and fluid-saturation temperatures, respectively, in °C. This is the correlation form for nucleate pool boiling, similar to that developed by Stephan and Abdelsalam (1980). The constants in Eq. 3 obtained from curve fits to the experimental data, and for the Stephan and Abdelsalam correlation for R-12, are given in Table 3.

In Fig. 15, the developed predictive equations for the circular-tube and rectangular-channel data are used to compare the two channels in the broad nucleation-dominant region ($\Delta T_{sat} > 2.75°C$). The Stephan and Abdelsalam correlation, which successfully predicted previous small-circular-tube data over the range of test conditions with R-113 as the boiling fluid (Wambsganss et al. 1993), is also plotted. The results show that there is no significant geometry effect for the two channels tested, each of which has approximately the same hydraulic diameter. At lower values of wall superheat, the Stephan and Abdelsalam correlation significantly underpredicts the data.

As noted in the Introduction, Tran et al. (1993) suggested that heat transfer may be somewhat more efficient in a small rectangular channel than in a small circular channel of the same hydraulic diameter. This finding came from a comparison of rectangular-channel R-12 data and state-of-the-art correlations (including the Stephan and Abdelsalam correlation [1980] shown in Fig. 15) representing R-12 heat transfer in a circular channel. The Stephan and Abdelsalam correlation gave good predictions of small-channel R-113 data

Table 3. Correlation coefficients for R-12

Correlation	C_1	C_2	C_3	C_4
Rectangular Channel	0.665	2.45	847	0.592
Circular Channel	0.427	2.71	731	0.631
Stephan-Abdelsalam	0.0364	3.92	429	0.745

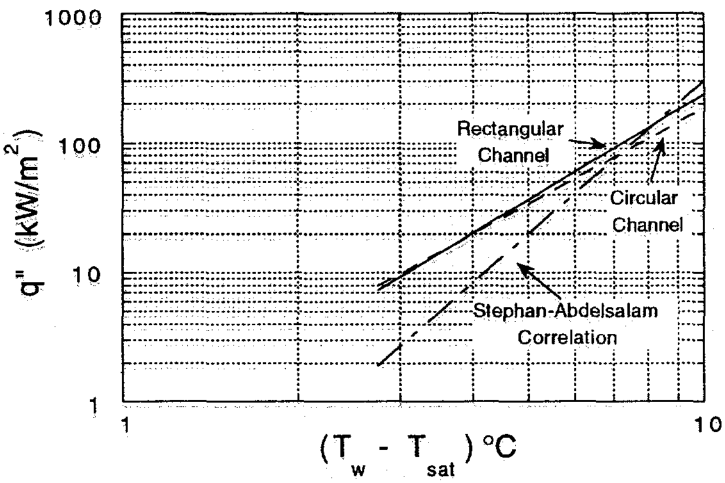

Fig. 15. Heat transfer behavior of small rectangular and circular channels with pool boiling prediction of Stephan and Abdelsalam (1980) ($\Delta T_{sat} > 2.75\,°C$)

(Wambsganss et al. 1993) and was used in the absence of small-circular-channel R-12 data. The ΔT_{sat} range of the comparison (Tran et al. 1993) was <5°C, which can be seen in Fig. 15 to be the range where the Stephan and Abdelsalam correlation is the poorest with the R-12 data of this study. It is also clear from Fig. 15 why the Stephan and Abdelsalam correlation predicted the R-113 data well when one recognizes that the wall superheat was above 7.2°C for all of the R-113 tests. Thus, the inference of some geometry enhancement on the heat transfer (Tran et al. 1993) was a consequence of the underprediction of small-circular-tube data by the Stephen and Abdelsalam correlation at wall superheats below 5°C. Based on R-12 data comparisons between both circular and rectangular channels (see Fig. 15), it has now been shown that the heat transfer rates are comparable.

5.3 Comparison with Large Tubes

As a result of the dominance of the nucleation mechanism to high qualities in small channel boiling, the heat transfer coefficients differ from those expected for large channels with the same mass flux. Comparisons were made with three large-tube correlations developed predominantly for refrigerant flow boiling, i.e., Kandlikar (1991), Jung and Radermacher (1991), and Liu and Winterton (1990). The data selected for the comparisons are shown in Fig. 16 and are from the 2.46 mm circular tube with R-12. The triangular symbols represent measurements made at a mass flux of 250 kg/m^{2}s with ΔT_{sat} < 3.5°C; they fall in

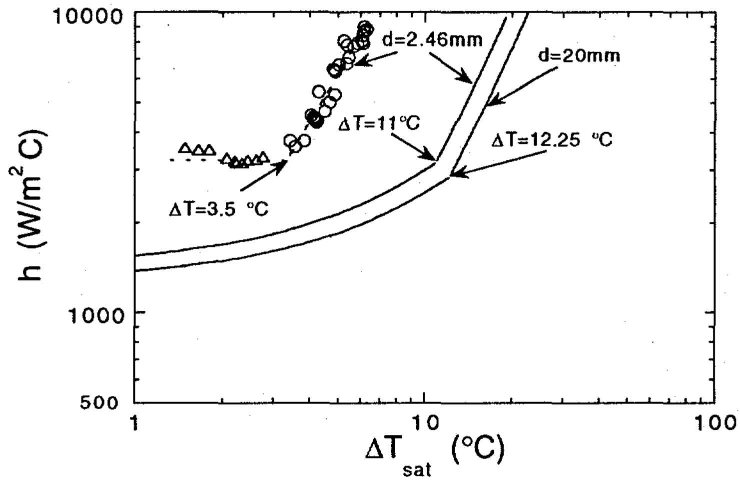

Fig. 16. Large tube comparison with circular channel data for R-12 using Kandlikar (1991) correlation; experimental data: ▲ *- convection region, G = 250 kg/m^{2}s;* ○ *- nucleation region*

the convection-dominant region. The circular symbols represent measurements in the nucleation-dominant boiling region, and here all data are plotted for G ≥ 250 kg/m^{2}s because the heat transfer coefficient has been shown to be independent of mass flux in this region. All large-tube comparisons were made against this data set.

The first large-tube comparison was made with the Kandlikar (1991) correlation that was developed from a large data base for relatively large-diameter tubes. The large-tube calculation shown in Fig. 16 is based on this correlation evaluated at an average quality of x = 0.5. Two predictions from the correlation with G = 250 kg/m^{2}s are given: one is for a large tube of 20 mm diameter, and the other is an extrapolation of the correlation to the tube diameter of the data, d = 2.46 mm. The two predictions are similar and fall well below the data. This shows significant heat transfer enhancement in the small channel at a given wall superheat.

The Kandlikar (1991) correlation exhibits a clear distinction between nucleation- and convection-dominant boiling regions. The transition between the two is seen in Fig. 16 as the abrupt change in slope of the calculations occurring at ΔT_{sat} = 11 and 12.25°C for the two diameters. The data show this transition at ΔT_{sat} = 3.5°C. The large-tube correlation predicts convection-dominant heat transfer and low heat transfer coefficients up to wall superheats of 11°C, while the small tube data show the heat transfer coefficient rising sharply in the nucleation-dominant region starting at $\Delta T_{sat} = 3.5°C$. (A value of $\Delta T_{sat} > 2.75°C$ has been used previously as a general criterion for the nucleation-dominant region. More accurately, the transition-temperature difference is a function of the mass flux as shown in Fig. 14 and occurs at $\Delta T_{sat} \approx 3.5°C$ at G = 250 kg/m^{2}s, as shown in Fig. 16.)

The effect of quality, used to calculate the heat transfer coefficients of Fig. 16 from the large-tube correlation of Kandlikar (1991), was considered in Fig. 17. The data covered a quality range of 0.2 to 0.8, and three qualities, essentially covering the experimental range, were chosen for this comparison as x = 0.3, 0.5 and 0.8. The results shown in Fig. 17 exhibit significant differences in the heat transfer coefficient predictions for the three qualities, but the general conclusion is unchanged: the large-tube correlation significantly underpredicts small-channel heat transfer. Because the predictions using the lowest quality (x = 0.3) were closest to the small-channel data, x = 0.3 was used in the next two large-tube comparisons for conservatism.

The flow boiling correlation of Jung and Radermacher (1991) was based on data of many refrigerants in relatively large-diameter tubes. The correlation includes both a nucleation- and a convection-dominant term, and the change from one to the other is gradual. Comparisons between the predictions of this correlation and the small-channel data are given in Fig. 18. The quality of x = 0.3 was chosen for the correlation, and two tube diameters were included as in the

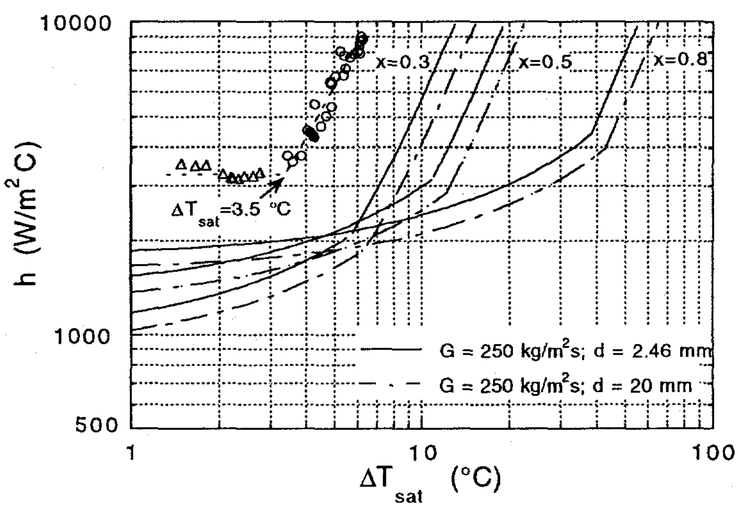

Fig. 17. Quality effect on large tube comparison with rectangular channel data; experimental data: ▲ - convection region, G = 250 kg/m^{2}s; ○ - nucleation region

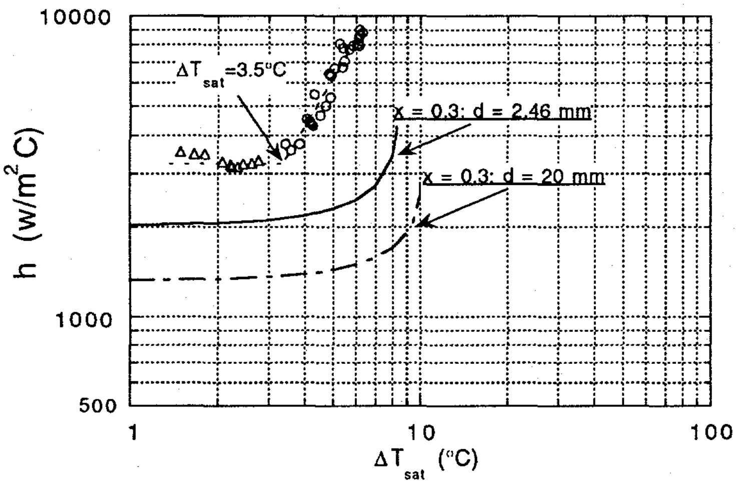

Fig. 18. Large tube comparison with circular channel data for R-12 using Jung and Radermacher (1991) correlation

results of Figs. 16-17. Although the correlation prediction of boiling mechanism transition is more gradual than in the Kandlikar correlation, it can be identified in the range of ΔT_{sat} = 8 to 10°C. This transition is lower than predicted by the Kandlikar correlation, but is still much higher than the experimental data transition of ΔT_{sat} = 3.5°C. As with the comparison with the Kandlikar correlation, the heat transfer coefficient data show significant enhancement compared to the predictions of the large-tube correlation of Jung and Radermacher (1991).

A final large-tube comparison was made with the flow boiling correlation of Liu and Winterton (1990). Like the other two large-tube, boiling-refrigerant correlations tested, the Liu and Winterton correlation includes explicit terms for both nucleation and convection mechanisms. The results of Fig. 19 show that the correlation predicts a very smooth transition from the convection- to the nucleation-dominant mechanism. The correlation predictions are slightly closer to the data than the other two correlations tested, but the data are still significantly underpredicted.

Wall superheats at the transition between the two boiling mechanisms were compared among the data and the correlations of Kandlikar (1991) and Jung and Radermacher (1991). The results are shown in Fig. 20 as a function of the quality used in the correlations. Both correlations exhibit the trends of Fig. 17, with the lowest wall superheats predicted at the lowest qualities. However, even these lowest predicted wall superheats were well above the small-channel data.

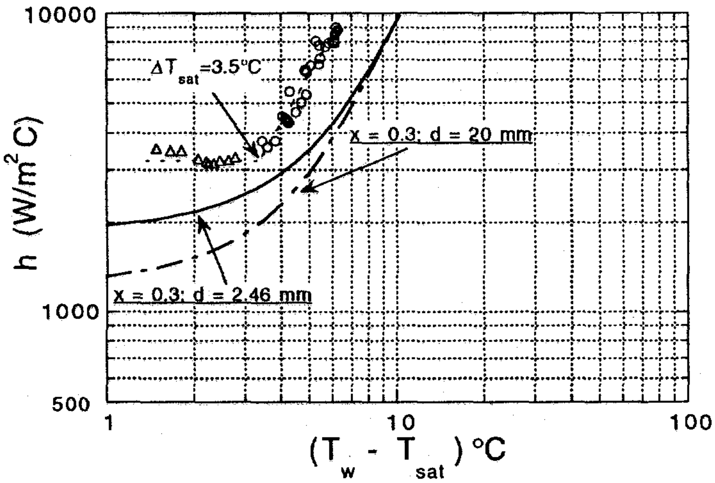

Fig. 19. Large tube comparison with circular channel data for R-12 using Liu and Winterton (1990) correlation

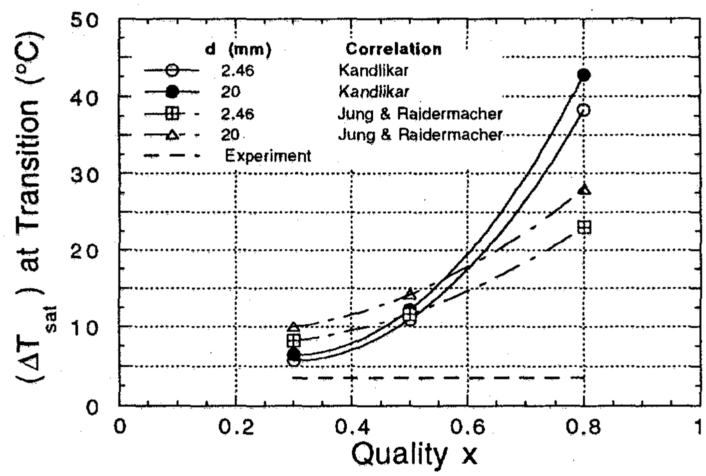

Fig. 20. Transition temperatures

5.4 Correlation of Data

Equation 3 was used to develop dimensional equations for the average heat transfer coefficient in the nucleation-dominant regime in the form

$$h = C_3 \, q''^{C_4}, \tag{4}$$

where h is in W/m^2°C, and q" is in kW/m^2. The coefficients C_3 and C_4, obtained by applying curve-fitting techniques, are given in Table 3 for the rectangular and circular tubes with R-12. The rectangular channel equation predicts 97% of the data within 15%, while the circular tube correlation predicts 98% of the data within 10%; see Figs. 21 and 22, respectively. (The data of Figs. 21 and 22 are for wall superheats above 2.75°C.) This illustrates that a nucleate pool boiling correlation form can be used to predict boiling heat transfer in small channels for wall superheats greater than 2.75°C. This form was followed in the development of a general heat transfer coefficient correlation for the nucleation-dominant regime.

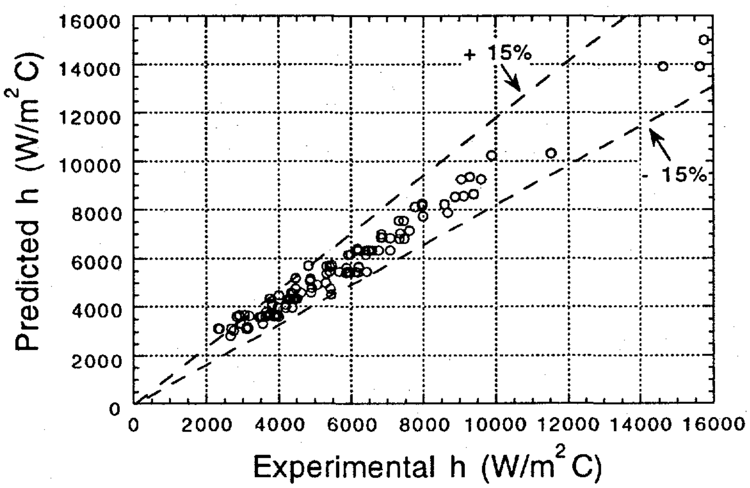

Fig. 21. Heat transfer predictions of Eq. 4 for rectangular channel (R-12)

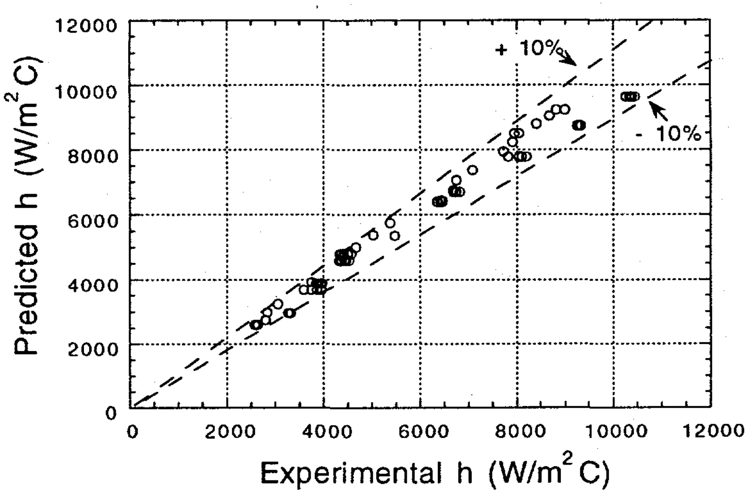

Fig. 22. Heat transfer predictions of Eq. 4 for circular tube (R-12)

As discussed above and shown in Figs. 21 and 22, the pool boiling heat transfer coefficient form of Eq. 4 predicted the small channel data well when coefficients were chosen specifically for each channel and fluid. The form of Eq. 4 was used by Stephen and Abdelsalam (1980) for larger tubes with fluid-specific coefficients, and it was shown to predict the small-tube R-113 and R-12 data well at higher wall superheats above 6°C. This form was used to correlate the small-tube data with wall superheats above 2.75°C for the three fluids tested (R-12, R-113 and R-134a) into a single predictive equation for the heat transfer coefficient; the data are given in the Appendix. Such a general correlation provides better flexibility in application.

The correlation of Lazarek and Black (1982) was based on R-113 boiling in a small-diameter (3 mm) tube. This correlation showed some success with the small-channel data of this study; it is based on the boiling and Reynolds numbers. The exponents of these two dimensionless parameters were such that when combined, the mass flux effect was very small and this allowed the correlation to follow the trends, if not the magnitude, of the small-channel nucleation-dominant data. However, because the dominant mechanism is nucleation rather than convection, the Reynolds number was replaced in this study with the Weber number to replace viscous effects with surface tension. Further accounting for fluid-property variations by the liquid-to-vapor density ratio, the heat transfer data were correlated in terms of dimensionless parameters as described below.

$$h = 840\left(Bo^2 We_\ell\right)^{0.3}\left(\frac{\rho_\ell}{\rho_v}\right)^{-0.4} \frac{kW}{m^2C}. \tag{5}$$

The predictions of Eq. 5 for all of the nucleation-dominant small-tube data of this study are compared to measurements in Fig. 23. Data from R-113, R-12 (circular and rectangular channels), and R-134a are shown separately. The comparison is considered to be very good, with most of the data predicted within a 15% random error band and no observable systematic errors. The product of the square of the boiling number with the Weber number introduces heat flux as the independent variable, while mass flux is eliminated. Property effects are correlated through the surface tension, latent heat of vaporization, and density ratio, all of which have been used in pool boiling correlation equations.

5.5 Comparison of R-12 and R-134a

Because R-134a was developed as a replacement refrigerant for R-12, it is useful to compare the heat transfer results for these two refrigerants directly. Experiments with the two refrigerants were conducted in the same 2.46-mm-

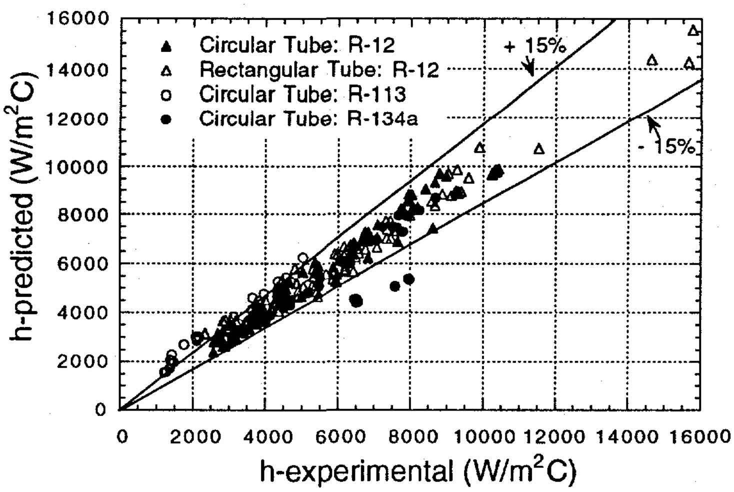

Fig. 23. Correlation of round tube data for three fluids at $\Delta T_{sat} > 2.75°C$

diameter round tube, making such a direct comparison possible. Shown in Fig. 24 are data from the R-134a experiments in the nucleation-dominant boiling heat transfer regime. The two lines plotted were shown previously (see Figs. 9 and 13) to represent the data for each fluid. The test results indicate that in the nucleate boiling region, heat flux (and thus heat transfer coefficient) is higher for R-134a than for R-12 at low values of wall superheat. However, the heat transfer coefficients for the two fluids approach each other as wall superheat increases, so that at high values of wall superheat the R-12 heat transfer coefficient is greater than the R-134a coefficient. In larger channels, the dominant heat transfer mechanism is convective boiling, and the heat transfer coefficient for R-134a has been determined to be greater than that for R-12 at comparable conditions.

6 Summary and Conclusions

Boiling heat transfer was measured with R-12 and R-134a in a small circular channel (d = 2.46 mm) over a substantial range of heat flux, mass flux, and quality. At all but the lowest wall superheats, heat transfer was found to be dependent on heat flux rather than on mass flux. This condition had been found previously in a small rectangular channel (Tran et al. 1993) with R-12 and in a small circular channel with R-113 (Lazarek and Black 1982; Wambsganss et al. 1993). The implication is that the nucleation mechanism dominates over the convective mechanism in small-channel evaporators over the full range of qualities (precritical heat flux qualities of 0.2 to 0.8); this is contrary to situations

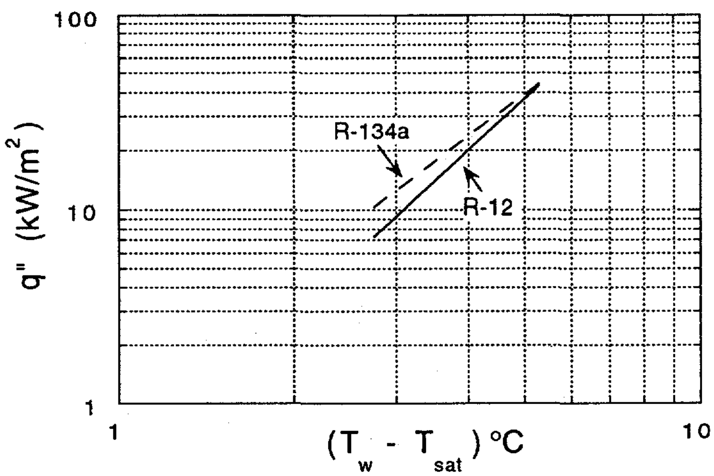

Fig. 24. Heat transfer behavior of R-134a and R-12 in nucleation-dominant region in 2.46-mm-diameter round tube

in larger channels where the convective mechanism dominates at qualities typically >0.2. This mechanism contributed to the finding that small-channel heat transfer exhibited an enhancement over predicted large-channel results.

Experiments were also conducted at very low wall superheats where, for ΔT_{sat} <≈2.75°C, the convection-dominant region was measured. Here, heat transfer was dependent on mass flux, not on heat flux. The transition between regions of nucleation- and convection-dominance was found to be rather sharp and occurred at significantly lower values of ΔT_{sat} than predicted for larger-diameter tubes. This result also contributed to the heat transfer enhancement in small channels relative to that in larger channels.

Circular tube data for R-12, R-134a, and R-113 in the nucleation-dominant region were correlated by a nondimensional form of the Stephan and Abdelsalam equation (Stephan and Abdelsalam, 1980) for pool boiling, where the heat transfer coefficient depends on heat flux rather than mass flux. The original Stephen and Abdelsalam correlation was found to predict small-channel data well in a range of wall superheats from about 6 to 9°C.

Two other comparisons were made among the experiments of this study. First, very little difference was found in the heat transfer coefficient between data in a small rectangular channel and in a round tube with the same hydraulic diameter; the same refrigerant (R-12) was used in both test series. Second, the heat transfer coefficient for R-134a was found to be higher than for R-12 at the same wall superheat; this is in line with findings in larger tubes.

Acknowledgments

This work was supported by the U.S. Department of Energy, Energy Efficiency and Renewable Energy, Office of Industrial Technologies, under Contract W-31-109-Eng-38. The work also represents a U.S. contribution to the International Energy Agency (IEA) program on Research and Development in Heat Transfer and Heat Exchangers.

The authors thank Joseph A. Jendrzejczyk for technical contributions during the course of the work, Roger K. Smith for his contributions in fabricating and instrumenting the experiment, and Joyce A. Stephens for preparing the figures and overall manuscript for publication.

References

Carey, V. P., and Mandrusiak, G. D., 1986, "Annular Film-Flow Boiling of Liquids in a Partially Heated, Vertical Channel with Offset Strip Fins," Intl. J. Heat Mass Transfer 29(6), 927-939.

Chen, C. C., and Westwater, J. W., 1984, "Application of the Local Assumption for the Design of Compact Heat Exchangers for Boiling Heat Transfer," ASME J. Heat Transfer 106, 204-209.

Galezha, V. B., Usyukin, I. P., and Kan, K. D., 1976, "Boiling Heat Transfer with Freons in Finned-Plate Heat Exchangers," Heat Transfer–Soviet Research 8(3), 103-110.

Jung, D. S., and Radermacher, R., 1991, "Prediction of Heat Transfer Coefficient of Various Refrigerants during Evaporation," ASHRAE Trans. 97(2), Paper No. 3492.

Kandlikar, S. G., 1991, "A Model for Correlating Flow Boiling Heat Transfer in Augmented Tubes and Compact Evaporators," ASME J. Heat Transfer 113, 966-972.

Lazarek, G. M., and Black, S. H., 1982, "Evaporative Heat Transfer, Pressure Drop and Critical Heat Flux in a Small Vertical Tube with R-113," Intl. J. Heat Mass Transfer 25(7), 945-960.

Liu, Z., and Winterton, R. H. S., 1990, "Wet Wall Flow Boiling Correlation with Explicit Nucleate Term," Multiphase Transport and Particulate Phenomena 1, T. Nejat Veziroglu, ed., Hemisphere Publishing Corp., New York, 419-432.

Mandrusiak, G. D., Carey, V. P., and Xu, X., 1988, "An Experimental Study of Convective Boiling in a Partially Heated Horizontal Channel with Offset Strip Fins," ASME J. Heat Transfer 110, 229-236.

Mandrusiak, G. D., and Carey, V. P., 1989, "Convective Boiling in Vertical Channels with Different Offset Strip Fin Geometries," ASME J. Heat Transfer 111(1), 156-165.

Panchal, C. B., 1984, "Heat Transfer with Phase Change in Plate-Fin Heat Exchangers," Heat Transfer–Niagara Falls 1984, N. M. Farukhi, ed., AIChE Symposium Series 80(236) 90- 97.

Panchal, C. B., 1989, "Analysis of Flow Boiling of Ammonia and R-114 in a Matrix Heat Exchanger," Heat Transfer–Philadelphia, 1989, S. B. Yilmaz, ed., AIChE Symposium Series 85(269), 293-300.

Panitsidis, H., Gresham, R. D., and Westwater, J. W., 1975, "Boiling of Liquids in a Compact Plate-Fin Heat Exchanger," Intl. J. Heat Mass Transfer 18, 37-42.

Peng, X. F., and Wang, B.-X., 1993, "Forced Convection and Flow Boiling Heat Transfer for Liquid Flowing through Microchannels," Intl. J. Heat Mass Transfer 36(14), 3421-3427.

Robertson, J. M., 1979, "Boiling Heat Transfer with Liquid Nitrogen in Brazed-Aluminum Plate-Fin Heat Exchangers," Heat Transfer–San Diego 1979, AIChE Symposium Series 75(189), 151-164.

Robertson, J. M., 1983, "The Boiling Characteristics of Perforated Plate-Fin Channels with Liquid Nitrogen in Upflow," Heat Exchangers for Two-Phase Applications, HTD-Vol 27, J. B. Kitto, Jr., and J. M. Robertson, eds., ASME, New York, 35-40.

Robertson, J. M., and Wadekar, V. V., 1988, "Boiling Characteristics of Cyclohexane in Vertical Upflow in Perforated Plate-Fin Passages," Heat Transfer–Houston 1988, AIChE Symposium Series 84(263), 120-125.

Shah, R. K., 1986, "Classification of Heat Exchangers," Heat Exchangers: Thermal-Hydraulic Fundamentals and Design, S. Kakac, A. E. Bergles, and F. Mayinger, eds., Hemisphere Publishing Corp., Washington, DC, 9-46.

Stephen, K., and Abdelsalam, M., 1980, "Heat Transfer Correlations for Natural Convection Boiling," Intl. J. Heat Mass Transfer 23, 73-87.

Tran, T. N., Wambsganss, M. W., France, D. M., and Jendrzejczyk, J. A., 1993, "Boiling Heat Transfer in a Small, Horizontal, Rectangular Channel," Heat Transfer–Atlanta 1993, AIChE Symposium Series 89(295), 253-261.

Wadekar, V. V., 1992, "Flow Boiling of Heptane in a Plate-Fin Heat Exchanger Passage," Compact Heat Exchangers for Power and Process Industries, HTD-Vol. 201, ASME, New York, 1-6.

Wambsganss, M. W., France, D. M., Jendrzejczyk, J. A., and Tran, T. N., 1993, "Boiling Heat Transfer in a Horizontal Small-Diameter Tube," ASME J. Heat Transfer 115(4), 963-972.

Yung, D., Lorenz, J. J., and Panchal, C., 1980, "Convective Vaporization and Condensation in Serrated-Fin Channels," Heat Transfer in OTEC Systems, HTD Vol. 12, W. L. Owens, ed., ASME, New York, 29-37.

Appendix: Small Channel Flow Boiling Data

Table A.1. Circular Tube (d = 2.92 mm); R-113

Small Channel Boiling Data
Tube geometry: Circular
Tube material: Stainless steel
Hydraulic diameter: 2.92 mm
Fluid: Refrigerant R-113

Run No.	P (kPa)	G (kg/m^2s)	q" (kW/m^2)	T_w-T_{sat} (°C)	h ($W/m^2°C$)	Bo	We
52	162	242	25.3	11.55	2190	0.00075	8.17
53	171	242	46.3	12.05	3838	0.00139	8.33
54	172	242	55.4	12.78	4345	0.00166	8.33
63	145	400	68.3	13.13	5198	0.00122	21.51
64	155	300	44.7	12.33	3624	0.00107	12.39
65	164	300	63.3	13.49	4701	0.00152	12.61
66	138	200	27.0	12.80	2113	0.00096	5.31
67	138	200	27.0	12.77	2116	0.00096	5.31
68	143	200	41.8	13.34	3132	0.00149	5.37
69	158	50	10.1	7.56	1362	0.00146	0.35
70	156	50	8.8	7.24	1225	0.00126	0.34
71	157	100	21.5	12.32	1749	0.00155	1.38
72	160	100	25.5	12.19	2098	0.00184	1.39
73	158	100	16.3	11.48	1424	0.00117	1.39
74	129	50	16.5	11.62	1429	0.00234	0.32
75	131	50	14.2	10.21	1412	0.00201	0.33
76	133	50	10.1	8.02	1276	0.00143	0.33
77	130	100	16.4	11.83	1394	0.00116	1.30
78	131	100	30.0	14.22	2115	0.00213	1.31
79	139	200	61.9	15.64	3963	0.00220	5.32
80	144	242	74.9	16.43	4573	0.00221	7.87
81	150	300	90.8	18.24	5040	0.00216	12.24
83	151	50	13.2	9.10	1475	0.00189	0.34
84	156	200	53.0	14.59	3656	0.00190	5.52
85	163	242	63.5	14.75	4347	0.00189	8.19
86	161	150	44.4	11.91	3779	0.00213	3.13
87	154	150	34.8	10.71	3258	0.00167	3.09

Table A.2. Circular Tube (d = 2.46 mm); R-12

Small Channel Flow Boiling Data
Tube geometry: Circular
Tube material: Brass
Hydraulic diameter: 2.46 mm
Fluid: Refrigerant R-12

Run No.	P (kPa)	G (kg/m^2s)	q" (kW/m^2)	T_w-T_{sat} (°C)	h (W/m^2°C)	Bo	We
B106	845	276	18.4	4.13	4455	0.000400	18.73
B107	858	194	18.4	4.16	4427	0.000568	9.36
B108	853	223	18.4	4.21	4362	0.000494	12.33
B109	849	243	18.4	4.12	4467	0.000453	14.63
B110	830	280	18.4	4.12	4457	0.000394	19.02
B111	825	251	18.4	4.14	4437	0.000441	15.19
B112	822	236	18.4	4.24	4335	0.000468	13.42
B113	813	210	18.4	4.20	4372	0.000527	10.50
B114	809	206	18.4	4.12	4466	0.000537	10.12
B119	826	243	18.3	4.04	4537	0.000452	14.33
B120	835	243	23.5	4.28	5477	0.000579	14.46
B122	815	180	7.4	2.38	3114	0.000247	7.72
B123	837	150	7.4	2.34	3173	0.000295	5.52
B124	822	121	7.4	2.36	3145	0.000366	3.54
B125	812	92	7.4	2.48	2992	0.000483	2.02
B128	846	499	42.3	5.22	8105	0.000509	61.41
B129	853	400	42.3	5.26	8046	0.000635	39.71
B130	864	596	42.3	5.16	8197	0.000426	89.03
B131	814	278	12.9	3.26	3952	0.000278	18.45
B132	820	277	12.9	3.25	3964	0.000279	18.47
B133	827	241	12.9	3.34	3859	0.000321	14.08
B134	821	213	12.9	3.43	3758	0.000363	10.91
B135	835	592	42.3	5.40	7830	0.000430	85.67
B136	824	176	7.5	2.59	2880	0.000254	7.48
B137	807	148	7.4	2.59	2871	0.000302	5.18
B138	854	792	55.5	6.29	8813	0.000422	155.72
B139	841	691	55.5	6.17	8994	0.000484	117.28
B140	832	399	31.2	4.83	6464	0.000471	38.77
B141	828	396	31.2	4.86	6422	0.000475	37.98
B142	824	321	26.2	4.88	5372	0.000492	24.95

Table A.2 (Cont'd)

B143	819	292	23.6	4.69	5032	0.000487	20.51
B144	815	263	21.0	4.49	4674	0.000481	16.56
B145	812	234	18.3	4.25	4322	0.000472	13.08
B146	819	191	14.4	3.83	3751	0.000452	8.76
B147	820	148	10.6	3.45	3063	0.000428	5.28
B148	818	134	9.3	3.29	2839	0.000419	4.29
B148a	818	134	9.3	3.29	2836	0.000419	4.29
B149	821	119	8.1	2.91	2804	0.000409	3.44
B149a	821	119	8.1	2.93	2785	0.000409	3.44
B150	823	684	51.3	6.10	8413	0.000454	112.73
B151	830	781	53.6	6.17	8680	0.000414	148.26
B152	829	568	48.7	6.13	7947	0.000518	78.38
B153	828	566	48.7	6.06	8047	0.000520	77.59
B154	826	527	46.2	5.84	7912	0.000530	67.13
B155	821	488	43.8	5.67	7723	0.000542	57.35
B156	812	430	38.7	5.45	7094	0.000544	44.08
B157	810	410	36.3	5.37	6756	0.000534	40.12
B158	803	390	33.7	5.04	6682	0.000521	36.13
B159	807	207	12.8	3.58	3583	0.000373	10.19
B160	810	105	5.8	2.28	2533	0.000329	2.64
B161	821	91	5.8	2.61	2222	0.000381	1.99
B162	815	63	4.5	2.49	1800	0.000428	0.94
B163	814	63	4.5	2.47	1814	0.000428	0.94
B164	835	399	31.2	4.86	6423	0.000471	38.87
B165	786	664	31.1	4.89	6366	0.000284	102.85
B166	844	617	31.2	4.84	6437	0.000304	93.57
B167	842	617	31.2	4.82	6467	0.000304	93.43
B168	841	695	31.2	4.83	6452	0.000270	118.62
B169	830	498	31.2	4.91	6346	0.000377	60.16
B170	826	497	31.2	4.91	6352	0.000378	59.73
B171	834	173	7.5	2.85	2624	0.000258	7.32
B171a	830	173	7.5	2.85	2625	0.000259	7.28
B172	824	173	7.5	2.83	2644	0.000259	7.21
B173	819	144	7.5	2.84	2625	0.000311	4.97
B174	816	116	7.5	2.90	2573	0.000385	3.24
B175	823	89	7.5	2.91	2569	0.000504	1.90
B176	829	89	7.5	2.87	2605	0.000504	1.91
B195	822	121	33.4	5.00	6682	0.001665	3.53

Table A.2 (Cont'd)

B196	817	150	33.4	4.95	6760	0.001346	5.38
B197	814	150	33.4	4.96	6736	0.001345	5.39
B198	809	179	33.4	4.89	6821	0.001124	7.64
B199	819	74	19.6	4.52	4337	0.001607	1.30
B200	817	75	19.6	4.50	4359	0.001578	1.34
B201	813	92	19.6	4.44	4422	0.001289	2.01
B202	808	106	19.6	4.35	4508	0.001117	2.67
B203	804	120	19.6	4.29	4576	0.000985	3.42
B204	813	120	14.0	3.54	3969	0.000702	3.45
B205	811	106	14.0	3.55	3951	0.000796	2.68
B206	808	92	14.0	3.61	3892	0.000920	2.00
B207	824	63	14.0	3.64	3852	0.001330	0.97
B208	822	253	50.8	5.49	9255	0.001209	15.49
B209	819	268	50.8	5.46	9297	0.001142	17.32
B210	815	268	50.7	5.44	9329	0.001142	17.22
B211	810	297	50.7	5.49	9244	0.001031	21.06
B212	807	326	50.7	5.48	9249	0.000940	25.31
B213	806	385	50.7	5.45	9313	0.000797	35.11
B216	823	386	59.5	5.70	10435	0.000931	35.89
B217	820	356	59.4	5.73	10355	0.001007	30.51
B218	816	326	59.4	5.73	10365	0.001100	25.53
B219	813	300	59.4	5.75	10327	0.001198	21.47
B220	810	264	59.4	5.72	10382	0.001358	16.67
B221	808	264	59.4	5.73	10371	0.001360	16.59
B222	800	238	59.4	5.79	10252	0.001513	13.33
B224	793	208	59.4	5.79	10258	0.001730	10.16
B236	787	76	3.9	1.37	2862	0.000310	1.33
B242	816	114	4.7	1.19	3917	0.000245	3.11
B243	817	114	5.0	1.44	3506	0.000264	3.11
B244	818	120	5.8	1.74	3353	0.000291	3.44
B245	818	120	6.3	1.85	3404	0.000314	3.45
B246	818	120	6.8	2.03	3344	0.000338	3.45
B247	818	152	7.1	2.21	3207	0.000279	5.55
B253	844	152	5.3	1.49	3544	0.000207	5.66
B254	843	152	5.8	1.66	3494	0.000228	5.66
B255	843	152	6.3	1.81	3499	0.000249	5.65
B256	843	152	6.8	2.07	3285	0.000268	5.65
B257	843	152	7.1	2.24	3174	0.000279	5.65

Table A.2. (Cont'd)

B258	843	152	7.9	2.45	3234	0.000311	5.65
B259	844	150	8.5	2.63	3246	0.000339	5.54
B260	844	152	9.2	2.77	3314	0.000362	5.66
B261	842	120	9.2	2.81	3269	0.000459	3.51
B262	840	119	7.8	2.45	3177	0.000390	3.50
B263	840	121	7.3	2.28	3197	0.000360	3.58
B264	838	72	6.2	2.58	2415	0.000519	1.26
B265	838	73	6.2	2.58	2413	0.000509	1.31
B266	837	72	5.6	2.27	2454	0.000466	1.25
B267	835	71	4.9	2.05	2406	0.000412	1.25
B268	835	71	4.4	1.83	2419	0.000370	1.25
B269	835	71	4.4	1.80	2467	0.000370	1.25
B270	834	71	3.6	1.33	2704	0.000300	1.24
B278	519	273	8.9	3.45	2574	0.000205	13.33
B279	521	272	10.2	3.58	2842	0.000236	13.19
B280	522	272	11.5	3.81	3026	0.000267	13.21
B281	523	269	13.0	4.08	3176	0.000304	12.92
B282	510	273	10.5	3.61	2898	0.000242	13.11
B283	512	272	12.7	3.95	3210	0.000294	13.14
B284	513	272	14.2	4.18	3406	0.000330	13.13
B285	514	271	15.2	4.30	3538	0.000355	13.00
B286	516	271	16.8	4.46	3768	0.000392	13.02
B287	517	272	18.2	4.65	3911	0.000422	13.17
B288	518	272	18.7	4.70	3982	0.000435	13.18
B293	517	359	26.6	5.34	4977	0.000469	22.98
B294	518	359	26.6	5.32	5005	0.000469	22.99
B295	521	435	35.3	5.91	5975	0.000515	33.81
B296	519	755	50.3	6.56	7656	0.000423	101.77
B297	514	553	43.1	6.32	6831	0.000496	54.30
B298	521	832	57.1	6.62	8626	0.000436	123.85
B299	521	831	57.1	6.63	8612	0.000436	123.55

Table A.3. Circular Tube (d = 2.46 mm); R-134a

Small Channel Flow Boiling Data
Tube geometry: Circular
Tube material: Brass
Hydraulic diameter: 2.46 mm
Fluid: Refrigerant R-134a

Run No.	P (kPa)	G (kg/m^2s)	q" (kW/m^2)	T_w-T_{sat} (°C)	h (W/m^2°C)	Bo	We
B306	415	356	36.8	5.70	6455	0.000541	24.05
B307	417	356	36.8	5.64	6527	0.000542	24.11
B311	414	391	35.2	5.42	6500	0.000472	29.03
B312	416	376	35.3	5.38	6555	0.000491	26.93
B313	421	394	43.5	5.75	7572	0.000579	29.75
B314	422	389	47.5	5.96	7961	0.000641	28.95
B315	425	391	47.5	5.97	7951	0.000638	29.40
B317	824	334	34.8	4.46	7804	0.000610	33.05
B318	825	284	34.8	4.49	7750	0.000718	23.83
B320	821	146	19.5	3.56	5480	0.000780	6.31
B321	817	146	19.5	3.56	5475	0.000779	6.28
B322	822	184	25.5	4.03	6329	0.000810	10.04
B323	819	212	25.7	4.15	6195	0.000707	13.29
B324	833	245	31.9	4.52	7056	0.000764	17.90
B325	827	303	36.1	4.73	7630	0.000698	27.28
B326	832	327	41.6	5.05	8241	0.000746	31.93
B327	837	360	46.0	5.29	8697	0.000750	38.83
B331	830	124	11.1	2.84	3902	0.000525	4.56
B332	826	126	15.8	3.52	4501	0.000737	4.69
B333	826	126	15.8	3.37	4698	0.000737	4.69
B334	828	162	15.8	3.44	4605	0.000573	7.80
B335	830	181	15.8	3.50	4527	0.000512	9.79
B336	829	244	21.3	3.87	5513	0.000511	17.75
B337	827	243	25.7	4.21	6108	0.000619	17.59
B338	828	276	25.7	4.24	6070	0.000545	22.72
B339	827	276	25.7	4.24	6064	0.000544	22.69
B340	827	274	31.9	4.69	6808	0.000682	22.34
B341	832	299	31.9	4.71	6778	0.000627	26.60
B342	831	326	31.9	4.65	6873	0.000574	31.76
B343	829	359	31.9	4.65	6864	0.000522	38.29
B345	831	396	36.1	5.00	7233	0.000534	46.88

Table A.3. (Cont'd)

B346	831	398	39.9	5.19	7679	0.000587	47.29
B348	828	476	31.9	4.61	6921	0.000392	67.45
B349	830	475	36.1	4.81	7506	0.000445	67.34
B350	827	473	39.9	5.05	7906	0.000494	66.46
B355	826	59	4.4	1.66	2676	0.000436	1.05
B356	828	58	4.8	1.69	2843	0.000483	1.00
B358	830	59	5.5	1.97	2779	0.000541	1.04
B360	828	114	6.1	1.62	3775	0.000315	3.85
B361	828	114	5.9	1.57	3753	0.000301	3.89
B362	828	115	7.0	1.84	3796	0.000357	3.91
B363	828	115	8.3	2.16	3849	0.000424	3.90
B364	829	114	9.5	2.47	3863	0.000490	3.87
B365	829	113	11.5	2.84	4030	0.000593	3.82
B366	830	112	13.9	3.09	4492	0.000723	3.77
B369	824	142	17.5	3.39	5177	0.000723	5.97
B370	820	142	14.7	3.13	4686	0.000603	5.96
B371	820	143	12.4	2.98	4144	0.000506	6.01
B382	841	72	5.9	1.96	3027	0.000482	1.57
B383	839	72	6.7	2.25	2963	0.000541	1.57
B384	829	72	5.5	1.88	2930	0.000447	1.56
B386	833	85	5.0	1.63	3100	0.000346	2.18
B387	836	85	5.9	1.82	3246	0.000406	2.19
B388	837	85	5.9	1.81	3262	0.000406	2.19
B389	839	85	7.0	2.18	3185	0.000479	2.18
B390	838	85	8.3	2.50	3319	0.000573	2.18
B391	831	142	6.2	1.55	3972	0.000255	6.00
B392	835	114	6.1	1.63	3777	0.000315	3.91
B393	836	114	7.2	1.91	3742	0.000370	3.87
B394	837	141	7.2	1.91	3750	0.000298	6.01
B395	837	141	8.4	2.21	3779	0.000348	5.97
B396	838	140	10.3	2.64	3895	0.000429	5.92
B397	837	113	10.3	2.76	3724	0.000534	3.81
B398	835	114	8.7	2.34	3694	0.000446	3.86
B399	833	86	6.7	2.05	3286	0.000459	2.22
B401	838	73	6.2	2.05	3010	0.000499	1.59
B402	838	72	8.2	2.46	3326	0.000663	1.57

Table A.4. Rectangular Tube (d_h = 2.40 mm); R-12

Small Channel Flow Boiling Data
Tube geometry: Rectangular
Tube material: Brass
Hydraulic diameter: 2.40 mm
Fluid: Refrigerant R-12

Run No.	P (kPa)	G (kg/m^2s)	q" (kW/m^2)	T_w-T_{sat} (°C)	h (W/m^2°C)	Bo	We
R485	841	84	5.6	2.05	2744	0.000402	1.67
R486	839	104	7.9	2.44	3229	0.000455	2.57
R499	845	145	10.8	2.43	4443	0.000443	5.07
R500	849	207	16.8	3.08	5442	0.000485	10.31
R501	851	289	23.4	3.64	6422	0.000484	20.15
R503	851	353	30.2	4.26	7081	0.000512	30.17
R504	865	489	43.4	5.00	8678	0.000532	58.66
R505	838	94	6.6	2.16	3042	0.000419	2.10
R506	841	124	9.4	2.98	3144	0.000451	3.68
R507	841	175	14.3	3.42	4195	0.000491	7.32
R508	841	237	19.5	3.84	5064	0.000491	13.50
R509	839	287	18.6	3.79	4902	0.000388	19.68
R510	841	287	13.6	3.43	3965	0.000284	19.71
R511	846	307	24.6	4.18	5881	0.000480	22.67
R512	853	421	35.7	4.86	7356	0.000510	42.86
R513	837	144	9.4	2.51	3738	0.000390	4.94
R514	831	145	7.0	1.85	3773	0.000287	5.01
R515	842	144	7.1	1.92	3694	0.000293	4.99
R516	837	210	10.1	2.83	3559	0.000287	10.50
R517	836	210	13.6	3.11	4381	0.000389	10.48
R518	783	286	23.0	3.93	5855	0.000486	18.56
R519	838	146	9.3	2.35	3978	0.000383	5.08
R520	850	287	23.3	3.76	6189	0.000485	19.91
R521	749	287	23.1	3.87	5970	0.000488	18.12
R522	947	289	23.4	3.83	6121	0.000480	22.03
R523	757	287	23.1	3.89	5932	0.000487	18.27
R524	819	355	17.4	3.76	4621	0.000294	29.65
R525	823	355	23.4	4.12	5666	0.000396	29.67
R526	846	311	24.7	3.99	6202	0.000477	23.19
R527	850	353	23.4	3.99	5869	0.000397	30.11
R528	847	354	23.4	3.95	5926	0.000396	30.10

Table A.4. (Cont'd)

R529	773	354	30.1	4.64	6489	0.000515	28.09
R530	808	354	30.0	4.56	6586	0.000512	29.06
R531	837	354	30.2	4.46	6770	0.000512	29.87
R531a	837	354	30.2	4.60	6557	0.000513	29.87
R532	812	353	30.1	4.85	6217	0.000514	29.09
R533	813	353	30.2	4.71	6403	0.000516	29.00
R536	839	354	23.3	4.30	5416	0.000395	29.85
R537	786	352	30.0	4.87	6173	0.000516	28.20
R538	828	353	17.4	4.01	4334	0.000296	29.38
R539	833	354	46.6	5.43	8581	0.000793	29.75
R540	834	289	34.3	5.04	6810	0.000715	19.87
R541	823	146	17.2	3.92	4394	0.000711	4.99
R542	835	105	11.6	3.31	3521	0.000666	2.61
R543	831	105	7.2	2.22	3236	0.000411	2.60
R545	820	278	22.8	4.30	5309	0.000493	18.19
R546	835	280	30.9	5.00	6171	0.000663	18.69
R547	825	325	20.7	4.26	4844	0.000382	24.99
R548	829	325	28.8	4.82	5976	0.000533	25.07
R549	842	381	46.9	5.88	7974	0.000742	34.71
R550	845	505	46.2	5.79	7978	0.000550	61.26
R551	850	504	57.9	6.23	9294	0.000692	61.32
R552	837	144	15.8	3.66	4313	0.000657	4.95
R553	837	174	15.8	3.67	4299	0.000543	7.24
R554	839	235	15.8	3.58	4409	0.000401	13.23
R555	825	115	11.6	3.34	3475	0.000605	3.12
R556	824	135	11.6	3.27	3543	0.000515	4.30
R557	823	176	11.6	3.20	3625	0.000395	7.27
R558	816	84	8.7	3.17	2754	0.000624	1.65
R559	817	94	10.1	3.44	2948	0.000649	2.06
R560	818	144	9.3	3.00	3087	0.000385	4.89
R561	814	144	12.6	3.45	3643	0.000522	4.87
R562	810	124	14.4	3.78	3812	0.000698	3.59
R563	814	175	21.1	4.34	4876	0.000729	7.13
R564	817	205	25.0	4.62	5407	0.000733	9.87
R565	820	287	25.0	4.71	5317	0.000526	19.30
R566	815	287	18.5	4.14	4473	0.000388	19.24
R567	839	236	28.6	4.84	5916	0.000727	13.35
R568	836	308	35.5	5.19	6838	0.000694	22.54
R569	834	351	25.4	4.63	5471	0.000434	29.34

Table A.4. (Cont'd)

R571	836	354	34.3	5.00	6859	0.000583	29.89
R572	848	423	56.7	6.28	9036	0.000808	43.19
R573	850	492	67.2	6.79	9891	0.000825	58.34
R578	826	146	9.4	3.00	3127	0.000386	5.00
R579	818	146	15.9	4.24	3747	0.000657	4.96
R580	831	176	11.6	3.28	3545	0.000396	7.38
R581	834	176	21.3	4.77	4469	0.000727	7.39
R582	816	207	25.1	5.21	4820	0.000732	10.03
R614	815	209	40.5	5.53	7316	0.001171	10.19
R615	812	208	40.5	5.44	7440	0.001176	10.06
R616	802	238	45.6	5.87	7767	0.001159	13.12
R617	820	239	56.8	5.91	9605	0.001438	13.36
R618	829	207	49.6	5.59	8877	0.001443	10.19
R619	822	177	42.1	5.27	7994	0.001436	7.35
R620	823	146	34.2	4.83	7081	0.001412	5.01
R621	838	125	28.6	4.46	6418	0.001371	3.75
R622	832	95	20.2	3.81	5304	0.001278	2.13
R623	814	85	17.4	3.56	4889	0.001230	1.68
R624	829	292	33.9	4.54	7473	0.000699	20.16
R625	825	292	33.9	4.62	7344	0.000700	20.08
R626	829	357	50.6	5.38	9393	0.000854	30.19
R627	834	357	68.3	5.92	11530	0.001154	30.26
R628	822	291	36.8	4.82	7624	0.000760	19.93
R629	814	291	49.8	5.47	9114	0.001035	19.78
R630	810	146	25.0	4.03	6202	0.001028	4.98
R631	832	146	18.5	3.41	5425	0.000757	5.08
R632	805	428	112.8	7.21	15648	0.001602	42.39
R633	814	426	113.1	7.73	14619	0.001613	42.40
R634	817	495	128.6	8.16	15759	0.001580	57.37
R635	813	70	16.7	4.17	4001	0.001435	1.14
R636	833	70	8.0	2.38	3362	0.000688	1.15
R637	827	95	13.7	3.28	4185	0.000866	2.13
R638	820	85	15.8	3.55	4459	0.001123	1.68
R639	817	105	15.8	3.51	4502	0.000906	2.57
R640	819	105	15.8	3.60	4386	0.000907	2.57
R641	823	125	15.8	3.50	4517	0.000759	3.68
R642	819	115	11.7	2.93	3992	0.000609	3.10
R643	816	105	11.7	2.93	3994	0.000669	2.57
R644	825	84	11.7	3.01	3880	0.000829	1.68

Table A.4. (Cont'd)

R645	815	64	11.7	3.35	3484	0.001091	0.97
R646	815	54	11.7	4.13	2835	0.001299	0.69
R647	813	44	7.7	2.88	2665	0.001042	0.46
R648	815	64	7.7	2.29	3360	0.000721	0.95
R649	814	54	7.7	2.37	3244	0.000851	0.68
R650	821	74	9.1	2.68	3403	0.000738	1.29
R651	817	64	9.1	2.89	3143	0.000850	0.96
R652	814	64	9.1	2.94	3094	0.000852	0.95
R653	816	54	9.1	3.40	2676	0.001012	0.68
R654	812	49	9.1	3.91	2331	0.001120	0.56
R655	810	49	9.1	3.88	2348	0.001121	0.56
R656	819	84	9.1	2.55	3567	0.000649	1.65
R657	817	74	12.2	3.29	3700	0.000989	1.28
R658	816	84	12.1	3.25	3739	0.000870	1.64
R659	814	104	12.1	3.12	3893	0.000701	2.53
R660	811	86	11.9	3.22	3685	0.000825	1.74
R661	807	74	11.8	3.72	3182	0.000958	1.28
R662	813	65	11.9	3.92	3050	0.001114	0.97
R663	806	55	11.9	4.12	2902	0.001320	0.69
R664	815	85	11.9	3.03	3943	0.000848	1.67
R666	816	85	11.5	3.35	3443	0.000817	1.68
R667	815	85	14.2	3.71	3815	0.001005	1.68
R668	823	85	15.7	3.71	4225	0.001113	1.69

Distribution for ANL-95/9

Internal

B. Arman
K. J. Bell
S. S. Chen
S. U. Choi
H. Drucker
D. M. France (10)
J. A. Jendrzejczyk
K. E. Kasza
C. A. Malefyt
T. J. Marciniak
N. T. Obot
C. B. Panchal
R. B. Poeppel
W. W. Schertz
R. K. Smith
T. N. Tran (10)
R. A. Valentin
M. W. Wambsganss (60)
R. W. Weeks
TIS Files

External

DOE-OSTI for distribution per UC-1423 (81)
ANL Libraries
  ANL-E (2)
  ANL-W
Manager, Chicago Field Office, DOE
Director, Technology Management Div., DOE-CH
D. L. Bray, DOE-CH
A. L. Taboas, DOE-CH
Energy Technology Division Review Committee:
  H. K. Birnbaum, University of Illinois, Urbana
  R. C. Buchanan, University of Cincinnati, Cincinnati, OH
  M. S. Dresselhaus, Massachusetts Institute of Technology, Cambridge, MA
  B. G. Jones, University of Illinois, Urbana
  C.-Y. Li, Cornell University, Ithaca, NY
  S.-N. Liu, Fremont, CA
  R. E. Smith, SciTech, Inc., Morrisville, NC